Remote reef cryptobenthic diversity: Integrating autonomous reef monitoring structures and in situ environmental parameters

Steyaert, M

10.3389/fmars.2022.932375
Frontiers in Marine Science
Frontiers Media SA

frontiers | Frontiers in Marine Science

TYPE Original Research
PUBLISHED 06 December 2022
DOI 10.3389/fmars.2022.932375

OPEN ACCESS

EDITED BY
Michael E. Hellberg,
Louisiana State University,
United States

REVIEWED BY
John Kenneth Pearman,
Cawthron Institute, New Zealand
Yin Cheong Aden Ip,
National Parks Board, Singapore
Jia Jin Marc Chang,
National University of Singapore,
Singapore, in collaboration with
reviewer YI

*CORRESPONDENCE
Margaux Steyaert
margaux.steyaert@biology.ox.ac.uk

SPECIALTY SECTION
This article was submitted to
Coral Reef Research,
a section of the journal
Frontiers in Marine Science

RECEIVED 29 April 2022
ACCEPTED 14 November 2022
PUBLISHED 06 December 2022

CITATION
Steyaert M, Lindhart M,
Khrizman A, Dunbar RB,
Bonsall MB, Mucciarone DA,
Ransome E, Santodomingo N,
Winslade P and Head CEI (2022)
Remote reef cryptobenthic diversity:
Integrating autonomous reef
monitoring structures and *in situ*
environmental parameters.
Front. Mar. Sci. 9:932375.
doi: 10.3389/fmars.2022.932375

Remote reef cryptobenthic diversity: Integrating autonomous reef monitoring structures and *in situ* environmental parameters

Margaux Steyaert[1,2]*, Mathilde Lindhart[3], Alexandra Khrizman[4], Robert B. Dunbar[4], Michael B. Bonsall[1], David A. Mucciarone[4], Emma Ransome[5], Nadia Santodomingo[6,7], Paige Winslade[8] and Catherine E. I. Head[1,2]

[1]Department of Zoology, University of Oxford, Oxford, United Kingdom, [2]Institute of Zoology, Zoological Society of London, London, United Kingdom, [3]Department of Civil and Environmental Engineering, Stanford University, Stanford, CA, United States, [4]Department of Earth System Science, Stanford University, Stanford, CA, United States, [5]Department of Life Sciences, Imperial College London, London, United Kingdom, [6]Department of Earth Sciences, The Natural History Museum of London, London, United Kingdom, [7]Institute of Earth Sciences, University of Lausanne, Lausanne, Switzerland, [8]School of Life Sciences, University of Essex, Colchester, United Kingdom

Coral reef sessile organisms inhabiting cryptic spaces and cavities of the reef matrix perform vital and varied functional roles but are often understudied in comparison to those on exposed surfaces. Here, we assess the composition of cryptobenthic taxa from three remote tropical reef sites (Central Indian Ocean) alongside a suite of *in situ* environmental parameters to determine if, or how, significant patterns of diversity are shaped by local abiotic factors. To achieve this, we carried out a point-count analysis of autonomous reef monitoring structure (ARMS) plate images and employed *in situ* instrumentation to recover long-term (12 months) profiles of flow velocity, wave heights, temperature, dissolved oxygen, and salinity, and short-term (3 weeks) profiles of light and pH. We recovered distinct environmental profiles between sampling sites and observed that ocean-facing reefs experienced frequent but short-lived cooling internal wave events and that these were key in shaping *in situ* temperature variability. By comparing temperature and wave height profiles recovered using *in situ* loggers with *ex situ* models, we discovered that global satellite products either failed to recover site-specific profiles or both over- and underestimated actual *in situ* conditions. We found that site choice and recruitment plate face (top or bottom) significantly impacted the percentage cover of bryozoans, gastropods, soft and calcified tube worms, as well as crustose coralline algae (CCA) and fleshy red, brown, and green encrusting macroalgae on ARMS. We observed significant correlations between the abundance of bryozoans, CCA, and colonial tunicates with lower mean temperature and higher mean dissolved oxygen profiles observed across sites. Red and brown encrusting macroalgae abundance correlated significantly with medium-to-high flow velocities and wave height profiles, as

well as higher pH and dissolved oxygen. This study provides the first insight into cryptobenthic communities in the Chagos Archipelago marine-protected area and adds to our limited understanding of tropical reef sessile communities and their associations with environmental parameters in this region. With climate change accelerating the decline of reef ecosystems, integrating analyses of cryptobenthic organisms and *in situ* physicochemical factors are needed to understand how reef communities, if any, may withstand the impacts of climate change.

KEYWORDS

autonomous reef monitoring structures, cryptobenthic, coral reef, community composition, temperature, internal waves, image analysis, coralnet

1 Introduction

Reef ecological studies often focus on the cover and composition of hard corals and fish species, but a large portion of diversity lies within benthic communities hidden in reef cryptic spaces (Klumpp et al., 1988; Appeltans et al., 2012; Leray and Knowlton, 2016). Scleractinian coral reefs are structurally diverse, with live and dead coral colonies forming a complex matrix of exposed surfaces and hidden cavities upon which many reef organisms rely. The surface area of hidden reef cavities significantly exceeds that of the exposed reef benthos, at times by a factor of eight (Scheffers et al., 2010), and can harbour highly diverse communities of sessile organisms including sponges, ascidians, bivalve molluscs, macroalgae, and annelids (Meesters et al., 1991; Richter et al., 2001). Many of these organisms are seldom seen on exposed reef surfaces, and the overall benthic biomass of these cryptic spaces is key for the cycling of nutrients and bacteria in tropical reef ecosystems (Scheffers et al., 2010; Pawlik and McMurray, 2020). These cavity communities and the environmental factors that influence their composition must therefore be considered when studying the functional outputs of coral reefs (de Goeij and Van Duyl, 2007; Kornder et al., 2021).

Our understanding of hidden sessile communities has advanced using genetic approaches, such as metabarcoding, in recent years (Vicente et al., 2021; Nichols et al., 2022). However, metabarcoding pipelines employing primers that target universal genetic regions have inherent sampling and amplification bias that currently limit our ability to quantify the abundance of taxonomic groups across marine benthic communities (van der Loos and Nijland, 2021). Image analysis has been a popular tool for estimating benthic cover, diversity, and recruitment success within cryptic cavities and surfaces of coral reefs (Scheffers et al., 2003; Scheffers et al., 2010; Kornder et al., 2021). Whilst molecular approaches such as metabarcoding can yield detailed information on the diversity of cryptobenthic organisms on autonomous reef monitoring structures (ARMS) (Pearman et al., 2018), image analysis enables researchers to estimate the percentage cover of individual taxa, therefore providing information on relative abundances on visible surfaces. In turn, such information can be used to study successional changes (Higgins et al., 2019) or estimate biovolume and biomass when images are converted to 3D photogrammetric modes (Kornder et al., 2021).

However, benthic organisms living in cryptic reef crevices are hard to access and photograph *in situ*, and thus, it is often challenging to study them without the risk of destroying or displacing the local reef matrix. ARMS were created to provide a standardised tool to both photograph and sample sessile and mobile reef cryptofauna for downstream image and genetic analysis (Zimmerman and Martin, 2004). These artificial devices are composed of stacked polyvinyl chloride (PVC) recruitment plates and have recently become a popular and successful way of studying cryptic reef invertebrates and their associated microbiomes (Al-Rshaidat et al., 2016; Pennesi and Danovaro, 2017; Carvalho et al., 2019; Pearman et al., 2019; Timmers et al., 2020; Cahyani, 2021; Steyaert et al., 2022). The standardised format of ARMS, along with widely available sampling and analysis protocols (Leray and Knowlton, 2015; Ransome et al., 2017), ensures that reef communities sampled across sites and regions can be compared using genetic or image-analysis methods (David et al., 2019; Obst et al., 2020; Pearman et al., 2020). Whilst a PVC material can bias the recruitment of benthic reef taxa (Mallela et al., 2017), and the short gaps between ARMS plates likely reduce predation/grazing pressure, the use of artificial recruitment devices such as ARMS is preferable to destructive sampling of the local reef matrix.

Abiotic factors such as water chemistry, wave exposure, currents, and tides have powerful influences on the shape, composition, and distribution of coral reef communities across multiple spatial scales (Gove et al., 2015; Steiner et al., 2018;

Davis et al., 2021). Parameters such as temperature and light availability in part determine the recruitment success, calcification, and growth rate of benthic organisms, whilst dissolved oxygen and pH are intrinsically linked to metabolic productivity across reef systems. Climate change threats to coral reef ecosystems include warming and ocean acidification, both of which are predicted to significantly degrade coral reefs around the globe in the coming decades (IPCC, 2022). Field and lab-based studies have focused on the response of individual non-coral sessile groups to changes in temperature and pH, including sponges (Bell et al., 2018), ascidians (Peck et al., 2015), crustose coralline algae (CCA) (Kroeker et al., 2013; Cornwall et al., 2020), bryozoans (Pecquet et al., 2017), soft corals (Lopes et al., 2018), and fleshy encrusting macroalgae (Diaz-Pulido and Barrón, 2020; Ho et al., 2021). With newly developed methods furthering our ability to record *in situ* biogeochemical fluxes across benthic reef communities (Roth et al., 2019), studies are now needed to determine how cryptobenthic communities as a whole respond to combined stressors.

Physical factors such as current velocity and wave forcing are also important for shaping the structure of coral reefs (Lange et al., 2021), but benthic reef communities have been shown to have non-linear threshold responses to changes in these parameters (Gove et al., 2015). Our understanding of the combined effect of physical and environmental factors on whole sessile communities within cryptic reef cavities is limited (but see Scheffers et al., 2010 and Timmers et al., 2021). Recent ARMS studies looking at cryptobenthic diversity across environmental gradients have used remote sensing data sourced from satellites and publicly available geographic information system (GIS) rasters (Pearman et al., 2018; Pearman et al., 2019; Pearman et al., 2020). Findings from these studies suggest that sea surface temperature (SST) is a key driver of bacterial communities (Pearman et al., 2019) and that a wide range of SST values negatively correlates with eukaryotic species richness (Pearman et al., 2020). Others could not determine whether spatial effects, determined by a lack of connectivity due to distance between sampling sites, or environmental conditions had an impact on ARMS sessile communities (David et al., 2019).

Indeed, global real-time products such as SST, altimetry-derived ocean currents, and modelled wave profiles are widely available and utilised to study large-scale trends across marine systems or as a substitute for *in situ* measurements when these are unavailable. However, the geographical resolution of satellite-based products is often coarse (one to tens of kilometres), and sea surface temperature products typically have longer temporal resolution than *in situ* loggers (Hu et al., 2021). In addition, there is often a disconnect between satellite microwave-based "skin" temperatures and actual water temperatures observed across several to tens of metres below the surface, due to the presence of vertical gradients and stratification (Pan et al., 2017). Internal wave events, which are characterised by intrusions of often cooler subsurface waters onto coral reefs, may be missed when relying on remote sensing models. For example, Colin and Johnston (2020), who compiled two decades of *in situ* temperature measurements from over 70 sites around the Republic of Palau, found that satellite-derived SST (sSST) was not able to capture an accurate picture of thermal variability on coral reefs due to the presence of internal waves. Internal waves are thought to be vital for bleaching mitigation (Safaie et al., 2018; Reid et al., 2019) and have been shown to reduce cumulative heat exposure by up to 88% on reefs across the Pacific during the 2015–2016 El Niño (Wyatt et al., 2020). On the other hand, when co-occurring with acidifying conditions, upwelling events can significantly increase reef bioerosion (Wizemann et al., 2018). The impact of internal waves and upwelling events on coral, kelp fish, and marine vertebrates has been studied and discussed (Lesser et al., 2009; DeCarlo et al., 2021), but to our knowledge, not with respect to whole cryptobenthic reef communities.

Uninhabited, protected, and remote shallow coral reefs are rare, but provide a unique opportunity to study the relationship between environmental factors and benthic communities free from anthropogenic stressors such as overfishing, seabed dredging, sound/chemical pollution, or coastal development, which have been shown to fundamentally alter the relationship between biological and physical factors on reefs (Williams et al., 2015). The Chagos Archipelago is a remote system of atolls located at the heart of the Indian Ocean, which has been uninhabited since the 1970s following the forced removal of local inhabitants. The archipelago is now part of a large no-take marine-protected area (MPA), and whilst the protection of these islands has been shown to benefit current populations of fish, turtles, and seabirds (Hays et al., 2020), shallow coral reefs across atolls have experienced bleaching events driven by climate change (Sheppard et al., 2017; Head et al., 2019; Lange and Perry, 2019). A recent review of climate change impacts on the Chagos Archipelago MPA highlights the urgent need for continuous monitoring of coral reef communities and local environmental variables across atolls (Koldewey et al., 2021). To our knowledge, no studies have investigated whole cryptobenthic communities from the reefs of the Central Indian Ocean, and few studies have investigated particular groups of cryptobenthic invertebrates from the Chagos Archipelago MPA (Head et al., 2018; Head et al., 2018; Hays et al., 2020).

Here, we present the first analysis of sessile cryptobenthic diversity and *in situ* environmental parameters for three shallow reef sites across the Chagos Archipelago MPA. We (1) use *in situ* measurements of abiotic factors including temperature, oxygen, light, pH, salinity, wave heights, and flow velocity to explore differences in environmental profiles between sites; (2) compare the percentage cover and composition of invertebrate communities using ARMS devices; and (3) investigate how environmental factors correlate with observed abundances of cryptobenthic taxa across reefs. Additionally, we (4) compare *in*

situ measurements of temperature and wave exposure to remote sensing data, to evaluate how representative these products are of local conditions. Overall, this study aims to advance our knowledge of cryptobenthic reef ecology in this understudied region by co-presenting and integrating analyses across fields of reef ecology, biogeochemistry, and physics.

2 Materials and methods

2.1 Study sites

Sampling sites (n=3) were distributed across two atolls of the Chagos Archipelago marine-protected area (MPA): one on the ocean-facing side of Moresby Island (Peros Banhos atoll), one on the ocean-facing side of Ile Anglaise (Salomon atoll), and another on the lagoonal side of Ile du Coin (Peros Banhos atoll) (Figure 1; Supplementary Table S1). For each site, benthic communities were sampled using triplicate autonomous reef monitoring structures (ARMS) and environmental parameters including temperature, salinity, dissolved oxygen, wave heights, depth, flow velocity, and photosynthetically active radiation (PAR) were recorded using *in situ* instrumentation (Figure 1).

2.2 Deployment, recovery, and processing of environmental data

Long-term environmental parameters were recorded at each site between 2018 and 2020, although recordings were asynchronous at times (Supplementary Table S3). The temperature was measured using an SBE56 temperature sensor (Sea-Bird Scientific, 30-s resolution) and an SBE37-SM/SMP MicroCAT (Sea-Bird Scientific, 10-min resolution). Flow velocity was measured using an Acoustic Doppler Profiler (1-MHz ADP; Nortek, 30-min resolution) in Ile Anglaise and an Acoustic Doppler Current P—filer (1200-KHz ADCP; RD Instruments, 20-min resolution) in Ile du Coin and Moresby. Dissolved oxygen (DO) was measured by miniDOT [PrecisionMeasurement Engineering (PME), 5–10–min resolution]. Salinity was measured by SBE37-SM/SMP MicroCAT (Sea-Bird Scientific, 10-min resolution), and

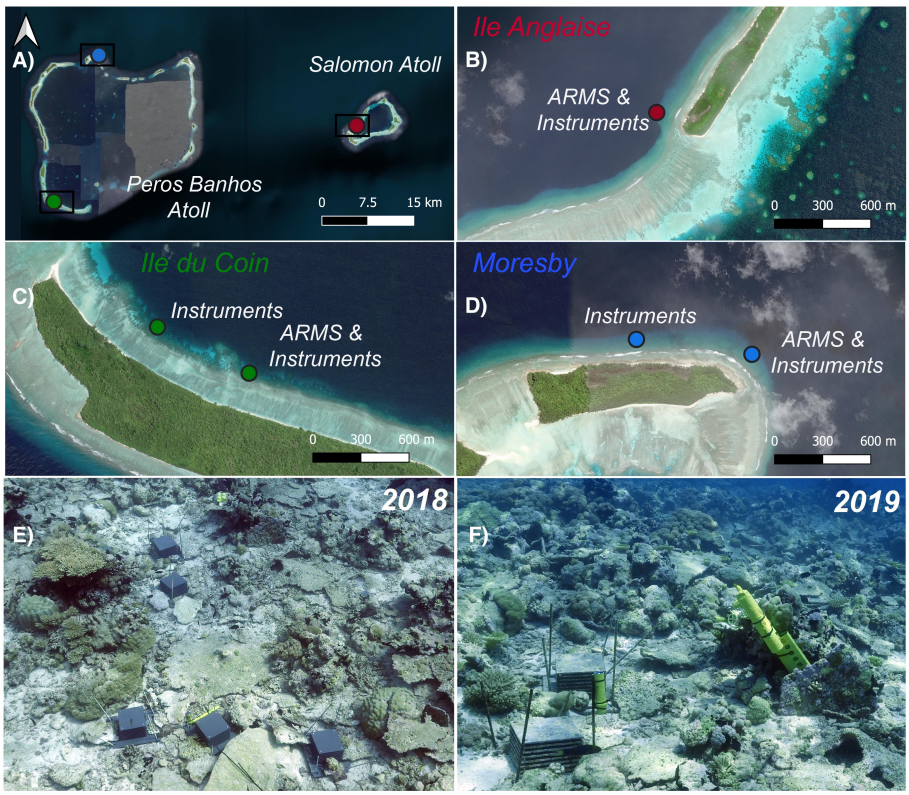

FIGURE 1
Maps displaying the location of **(A)** sampling sites across Peros Banhos and Salomon atolls in the Chagos Archipelago marine-protected area (MPA), **(B)** autonomous reef monitoring structures (ARMS) and environmental instruments at Ile Anglaise, **(C)** ARMS and environmental instruments at Ile du Coin, and **(D)** ARMS and environmental instruments at Moresby Island. **(E)** ARMS devices and environmental instruments at Ile Anglaise in 2018 following deployment and **(F)** ARMS devices and instruments at the same site in 2019.

pressure (waves) was measured by RBR Virtuoso (Ruskin, 1-Hz resolution) in Ile Anglaise and an RBR solo (Ruskin, 1 Hz) in Ile du Coin and Moresby. Long-term temperature, salinity, and dissolved oxygen measurements were taken directly adjacent to ARMS across all three sites (Figure 1). Flow velocity and wave heights were taken adjacent to ARMS at Ile Anglaise but were measured 500 to 700 m away from ARMS in Ile du Coin and Moresby (Figure 1). Additional details of individual instruments, deployment timelines, and calibration parameters recording these long-term variables can be found in Supplementary Table S4.

Leading up to the retrieval of ARMS in March 2019, short-term deployments (2 to 3 weeks) of the aforementioned parameters, along with pH and photosynthetic active radiation (PAR), were also conducted at each site. pH was recorded by SeaFET V2 pH logger (Sea-Bird Scientific, 10-s resolution) in Ile Anglaise and by SeapHOx V2 CTD-pH logger (Sea-Bird Scientific, 30-s resolution) at Ile du Coin and Moresby (Supplementary Table S5). Both instruments have an accuracy of 0.05 pH units and a precision of 0.004 units and were calibrated using collected discrete water samples at each site. PAR was measured by miniPAR [Precision Measurement Engineering (PME), 1-min resolution]. Short-term measurements were taken adjacent to ARMS at Ile Anglaise but were taken 500 to 700 m from ARMS for Ile du Coin and Moresby (Figure 1). Additional details of individual instruments, deployment timelines, and calibration parameters recording these short-term variables can be found in Supplementary Table S5.

Following Wyatt et al. (2020), the temperature time series was separated into high- and low-frequency signals, using the inertial frequency at −5.5° south as the cutoff, and temperature perturbations at higher frequencies are attributed to internal waves (IW). To determine the contribution of internal waves to overall temperature profiles, a time series was created where the internal wave signal is removed for Ile Anglaise and Moresby, labelled "Internal waves removed."

2.3 Satellite-derived sea surface temperature and modelled wave data

In situ data for wave heights and temperature were compared to NOAA's (National Oceanic and Atmospheric Administration) WaveWatch III wave model (WAVEWATCH III Development Group, 2016) and NOAA's (National Oceanic and Atmospheric Administration) Coral Reef Watch (CRW) (Liu et al., 2008) temperature observations for our three study sites. WaveWatch III (WWIII) simulates global wave characteristics at varying scales, and the available resolution around the Chagos Archipelago is to a 0.5°, equivalent to approximately 55 km. CRW provides daily sSST on a 5-km grid. *In situ* observations were compared to the WWIII output of significant wave height combining wind and swell, produced every 3 h. WWIII model output and daily sSST were available for the duration of *in situ* deployments of wave height and temperature loggers.

2.4 Deployment, recovery, and processing of autonomous reef monitoring structures

A total of nine ARMS were deployed across the three sampling sites in March 2018 at depths ranging from 5.9 to 9.3 m. Triplicate ARMS were collected from each site in March 2019 ($n = 9$). The use of triplicate units per sampling site, instead of duplicates, has been previously recommended in a study of ARMS communities from the Red Sea, as it was shown to significantly improve statistical power in the analysis of recruitment plate images (David et al., 2019). Each ARMS device is composed of nine square PVC plates (22.5 cm × 22.5 cm) stacked atop each other and attached to one larger base plate (35 cm × 45 cm). Between each plate are a series of alternating "open" and "closed" gaps created using round nylon spacers or long and short PVC cross spacers, thus creating multiple microhabitats. Each ARMS has a total of 17 colonisable plate "faces," referring to either the top (T) or bottom (B) side of each square plate (Supplementary Figure S1).

ARMS were retrieved on scuba and immediately submerged in a bin filled with filtered seawater and aquatic bubblers to maintain sessile communities. Each plate was carefully taken apart from the ARMS units by removing steel bolts, washers, and PVC crossbars, and each top and bottom plate face was photographed. For each face, a series of six close-up photographs were captured using a Nikon D810 camera (105-mm macro lens), then stitched together in Adobe Photoshop Lightroom Classic (version 9.2.1) to produce a single high-resolution image. Following photography, sessile communities were immediately subsampled and homogenised for downstream genetic analysis, the results from which are not presented in this study. All ARMS were processed and photographed on board an expedition vessel.

All final high-resolution plate images were exported in JPEG format with an image size of 6,000 × 6,000 pixels (240 pixels/in.). Labels of images contain the ARMS number, followed by the plate number (1 to 9 from top to lower plate) and the plate face (T or B). For instance, ARMS3_1B refers to the bottom side (B) of the uppermost plate (1) of the third ARMS device. Plate 9B lies flush with the base attachment plate and therefore, is not available for benthic recruitment.

2.5 Photo analyses of autonomous reef monitoring structures

The benthic composition of 139 ARMS plate images was analysed using CoralNet, an open-source cloud-based image-analysis website (coralnet.ucsd.edu). Five plate images from Ile

Anglaise were missing from our dataset, and to focus our analysis on communities within cryptic reef spaces, we did not analyse the top plate (plate 1T) on each of the nine ARMS, as it is the only plate face that is fully exposed and has been shown to harbour significantly different communities than other ARMS microhabitats (David et al., 2019). A list of identification groups based on NOAA's Coral Reef Ecosystem Program's (CREP) protocol was created to reflect the major taxonomic groups found in sessile tropical reef communities (Supplementary Table S2). A total of 225 annotation points were randomly generated on each ARMS plate image within a 15-row × 15-column grid format (one point randomly placed per cell). Identifications were made manually, and images were analysed in a randomised order across ARMS and sites.

2.6 Statistical analyses

One-way analysis of variance (ANOVA) tests were performed on individual long-term (*in situ* temperature, DO, flow velocity, and wave heights) and short-term (pH, salinity) environmental parameters between sampling sites, using the "rstatix" package (Kassambra, 2021). For each environmental parameter, 1,000 data points were randomly chosen for each site across overlapping instrument deployment periods. For each subset dataset, assumptions of data normality across sampling sites were checked by plotting model residuals and computing a Shapiro–Wilk test, and assumptions of homogeneity of variances were checked by plotting residual versus fitted plots. Only daytime values of PAR were retained and compared between sites. *Post-hoc* Tukey's tests were then used to perform pairwise comparison between sites. Plots summarising average diel cycles were then created for each parameter found to have significant differences in mean values across sites. The correlation between flow velocity and wave heights, as well as pH and DO, were investigated separately using Pearson's correlation analysis.

Live percentage cover was calculated as the percentage of counts assigned to live sessile taxonomic groups out of all counts observed on available space (i.e., excluding "unavailable" counts, which are characterised by any point falling outside of an ARMS plate or onto portions of plates obstructed by washers or crossbars). This was done to standardise the abundance of individual taxa between "open" and "closed" plate faces, as the latter has fewer counts on available space due to the presence of PVC crossbars during deployment. The mean values of the percentage cover of live sessile organisms were calculated for each site and across top/bottom plate faces. All plots of ARMS data were created using either the package "ggplot2" v3.3.5 (Wickham, 2016) or basic R plotting tools (R Core Team, 2022).

A series of univariate generalised linear models (GLMs) were used to investigate the relationship between live sessile percentage cover (%) with sites and plate faces, using the R package "MASS" v7.7.3.54 (Venables and Ripley, 2002). Percentage cover was transformed to proportional values (between 0 and 1) prior to running GLMs, and a quasi-binomial distribution was chosen to account for observed underdispersion (Gelman and Hill, 2006). *Post-hoc* Tukey's tests were used to determine significant patterns amongst explanatory variables.

Overall, community similarity between sites and plate faces was visualised using a non-metric multidimensional scaling (NMDS) approach using the R package "vegan" v2.5.7 (Oksanen et al., 2013), using Bray–Curtis distances. The distance matrix was created using the counts of sessile groups, except for groups "Hydrocorals" and "Corallimorphs," which were removed due to either low (n = 2 for hydrocorals) or no counts (n = 0 for corallimorphs). Top plate counts and bottom plate counts were merged for each ARMS device. Multivariate generalised linear modelling (GLM) was then used to determine the relationship between benthic group abundances and explanatory variables (plate face and site), using the *manyglm* function in the "mvabund" package (Wang et al., 2012), which uses row resampling to ensure correlations between taxa groups are taken into account when making community-wide and group-specific inferences. This method was used as a strong mean–variance relationship was observed across this study's benthic dataset (see Warton et al., 2012). Multivariate models with and without an interaction between the plate face and sites were computed, and the former was found to provide a better fit based on AIC Akaike Information Criterion values. A negative binomial distribution also provided a good model fit in a residual analysis and was therefore used to account for the overdispersion observed in our count dataset. Analyses of deviance were undertaken on multivariate and univariate model outputs using the *anova.manyglm* function, with a default PIT Probability Integral Transform-trap resampling parameter.

A distance-based redundancy ordination analysis (dbRDA) was used to determine the contribution of environmental parameters to the structure of ARMS cryptobenthic communities observed across sites, using Bray–Curtis distances with the *capscale* function in the "vegan" package v2.5.7 (Oksanen et al., 2013). The number of site replicates in this study limited our ability to simultaneously model the effect of all environmental variables with diversity patterns observed in our ARMS dataset, and therefore, we conducted individual dbRDAs on mean (i) *in situ* and *ex situ* temperature, (ii) pH and oxygen, and (iii) velocity and wave height. *Ex situ* wave values were not included in this analysis as the WaveWatch III model was unable to determine wave profiles between the Ile du Coin and Moresby sites. PAR and salinity were also not included in this analysis, as no difference was observed in the PAR profiles across sites and the significant profiles in salinity observed between sites were determined not to be biologically significant. ANOVA-like permutation-based tests were carried out to test the significance of each full model using the *permutest* function.

The significance of individual explanatory variables within each model was also tested using the *anova.cca* function. Ordination plots were then used to visualise modelled relationships between environmental factors and benthic communities for each model.

The *multipatt* function in the package "indicspecies" v1.7.9 (Cáceres and Legendre, 2009) was then used to determine the extent of correlation between sessile taxonomic groups and environmental parameters. Following our findings from the analysis of our environmental dataset (one-way ANOVAs and average diel plots), we categorised each site, or groups of sites, into regimes based on relatively significant differences observed between sites (Figure 2, see Sec. 2. Materials and methods). For flow velocity, we categorised Moresby as having a "high" regime, Ile Anglaise as "medium," and Coin as a "low" regime. For wave heights, Moresby was categorised as a high regime, Ile Anglaise as medium, and Ile du Coin as low. For *in situ* temperature, Ile du Coin was categorised as a high regime, and both Ile Anglaise and Moresby as low. For DO, Ile du Coin was categorised as low whilst both Ile Anglaise and Moresby were categorised as high. For pH, Ile du Coin was categorised as low, Moresby as medium, and Ile Anglaise as high. Finally, for PAR, we grouped Ile du Coin and Ile Anglaise sites together and categorised them as low, and categorised Moresby as high. This analysis was run on top and bottom plate face communities separately, and only results

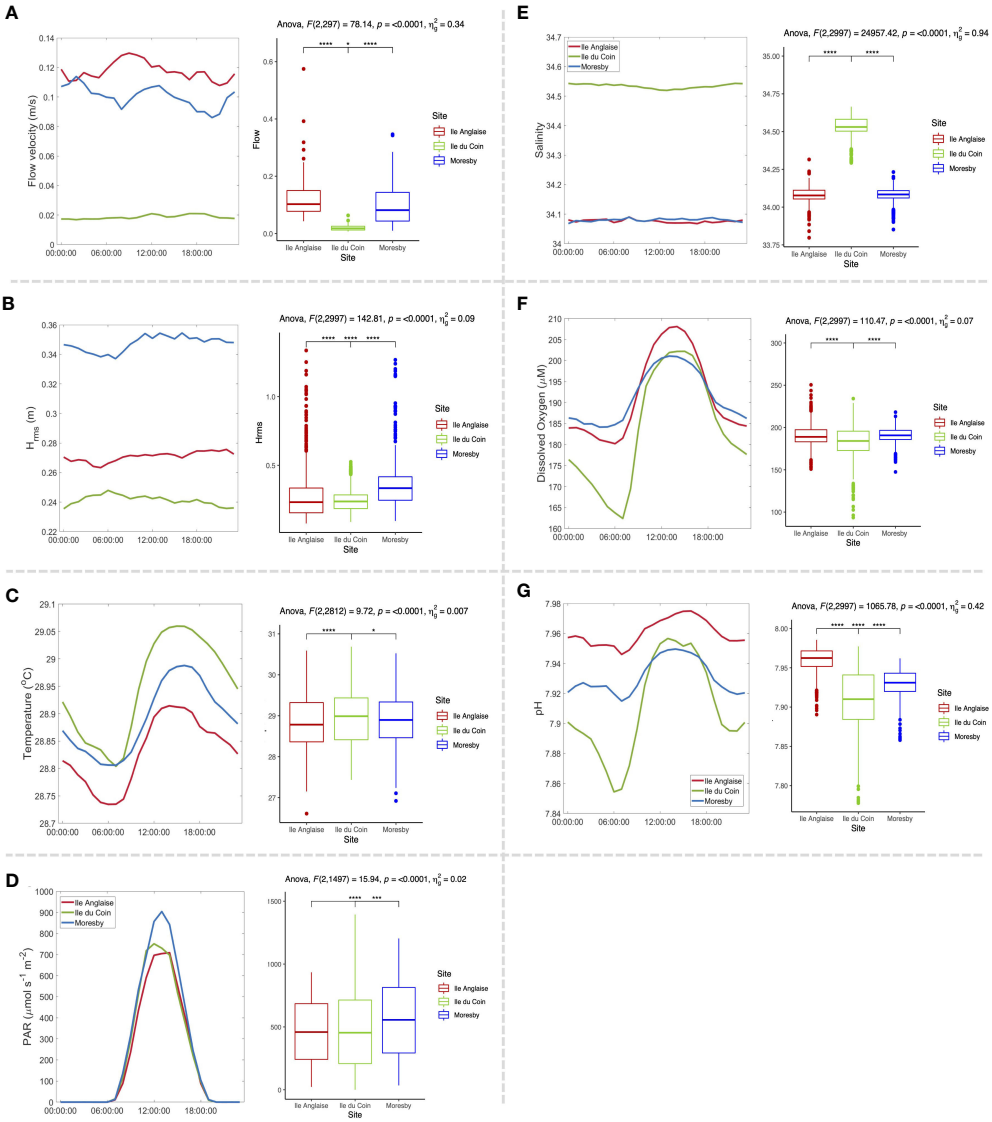

FIGURE 2
Average diel cycle plots for **(A)** flow velocity, **(B)** root-mean-square wave height, **(C)** in situ temperature, **(D)** photosynthetically active radiation (PAR), **(E)** salinity, **(F)** dissolved oxygen (DO), **(G)** pH, and, and boxplots displaying values across subset datasets for each parameter, along with corresponding one-way ANOVA test results [including *F*-statistic with degrees of freedom, *p*-value, and effect size (generalised eta squared (n_g^2)].

from taxa whose abundance was previously found to be significantly affected by plate face and site choice by multivariate GLMs were retained. The function parameter "r.g" was chosen to account for unequal group size (for the site) and to determine point biserial correlation coefficients.

3 Results

3.1 Environmental parameters

3.1.1 Tides, wave heights, and flow velocities

Tides were semidiurnal, and all sites had a similar tidal range of approximately 1 m (Supplementary Figures S2, 3). Limited wave forcing was observed in Ile du Coin, with root-mean-square wave heights (H_{rms}) varying between 0.07 and 0.57 m, and average (± sd) values of 0.23 (± 0.09) m across March–November 2019 (Figure 2; Supplementary Figure S2). In contrast, Ile Anglaise and Moresby reefs consistently experienced larger waves with root-mean-square wave heights of up to 1.40 and 1.33 m, respectively. On average, Moresby showed the highest average wave heights (0.35 ± 0.15 m), followed by Ile Anglaise (0.27 ± 0.16 m). Overall, average root-mean-square wave height values were significantly different between sites (ANOVA, F = 142.81, p-value < 0.001), but site choice accounted for only ~10% of the variance observed across this dataset (n_g^2 = 0.09).

Flow velocities were lower and less variable in the lagoonal reef (1.9 ± 1.0 cm/s; mean ± SD) compared to Moresby (10.1 ± 7.2 cm/s) and Ile Anglaise (11.6 ± 6.9 cm/s), over an annual period (Supplementary Figure S2). The mean flow velocities were also found to significantly differ between all three sites (ANOVA, F = 78.14, p-value < 0.001), and the site accounted for over a third of the variance observed (n_g^2 = 0.34) (Figure 2). A low positive correlation between flow and velocity was found in Ile du Coin (Pearson's coefficient = 0.215, p-value < 0.05) and Moresby (0.059, p-value < 0.05), whilst no correlation was observed between parameters in Ile Anglaise (0.003, p-value > 0.05) over overlapping instrument deployments.

3.1.2 Temperature

The *in situ* temperature profiles of the three sites were successfully recovered across April 2018 to January 2019 and March to April 2019 (Supplementary Figure S2). For all three sites, the maximum monthly mean (MMM) was 29.3°C. The average temperature (mean ± SD) in both ocean-facing reefs was similar (28.51°C ± 0.60 for Ile Anglaise, 28.57°C ± 0.58 for Moresby), with the lowest temperature recorded in Ile Anglaise (24.74°C on 15 October 2018). On average, the temperature was significantly higher in the lagoon-facing reef than in other sites (29.40°C ± 0.94) (ANOVA, F = 9.72, p-value < 0.001) (Figure 2), and the maximum temperature (30.98°C) was recorded there on 1 April 2019. Whilst a clear daily cycle was observed in Ile du Coin, a 24-h cycle of temperature variability was less clear in the two outer reefs (Figure 2; Supplementary Figure S3).

It was estimated that the site alone accounted for less than 1% of the variance observed in the subset temperature dataset (n_g^2 = 0.007). Events of cold intrusions, most likely caused by internal waves, were frequently detected in both outer-reef sites, during which significant drops in temperatures were observed, characterised by changes in hourly standard deviation temperature values (Figure 3). No internal waves were detected in Ile du Coin (Figure 3).

We determined that temperature values below 26.96°C and 27.22°C were attributable to internal wave events for the Ile Anglaise and Moresby sites, respectively. Overall, 0.20% of Moresby *in situ* temperature data was identified as potential internal wave events, compared to 0.42% of data points for Ile Anglaise, over the same period. Following the removal of internal wave signal from *in situ* data across these two sites, we find that whilst significant differences were still detected between reefs (ANOVA, F = 247.17, p-value < 0.001), the site was estimated to account for 14% of the variance observed (n_g^2 = 0.14), which is 20 times greater than what is estimated for the original *in situ* temperature dataset.

3.1.3 Photosynthetically active radiation, salinity, oxygen, and pH

The highest value of PAR (mean and daily max mean ± SD) was recorded in Moresby, with a total mean of 235.4 µmol photons/m^{-2} s^{-1} and a daily max mean of 1,579.5 µmol photons/m^{-2} s^{-1} (± 333.74). The lowest PAR was recorded in Ile Anglaise (total mean 189.3, daily max mean 1,089.1 µmol photons/m^{-2} s^{-1} ± 280.36), with an intermediate mean value in Ile du Coin (total mean 214.7, daily max mean 1,354.2 µmol photons/m^{-2} s^{-1} ± 313.33) (Supplementary Figure S3). Significant differences were observed between mean daytime PAR values across sites (ANOVA, F = 15.94, p < 0.001), but site choice was estimated to account for only 2% of the variance observed (n_g^2 = 0.02).

Higher salinity values (mean ± SD) were observed on average in Ile du Coin (34.53 ± 0.06 psu) than in Moresby (34.08 ± 0.04 psu) and Ile Anglaise (34.08 ± 0.04 psu), where values were identical. Overall, similar seasonal patterns were observed across all three sites, with a steady rise in salinity over the months of April to July (Supplementary Figure S2). Whilst statistically significant differences in mean values were observed across a subset of salinity data between ocean-facing sites and the lagoon-facing reef (ANOVA, F = 24,957.42, p < 0.001) (Figure 2), differences in these profiles are likely not biologically significant.

Dissolved oxygen (DO) concentration was lower in Ile du Coin on average (183.40 ± 18.71 µM) compared to Moresby (191.39 ± 8.57 µM) and Ile Anglaise (191.48 ± 12.88 µM) (Supplementary Figure S2). These differences in mean values were also found to be significantly different (ANOVA, F = 110.47, p <0.001), and the site was estimated to account for

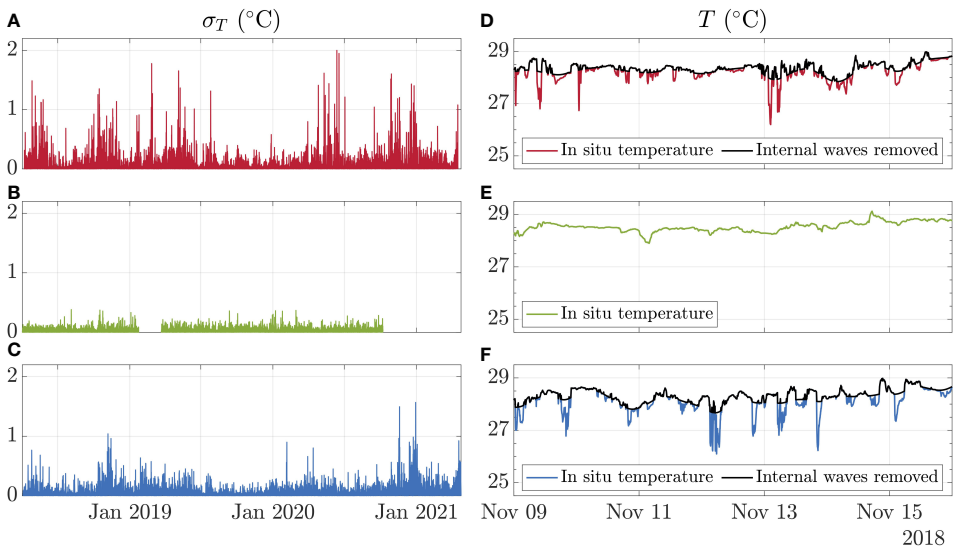

FIGURE 3
The hourly standard deviation of temperature across **(A)** Ile Anglaise (red), **(B)** Ile du Coin (green), and **(C)** Moresby (blue) between April 2018 and April 2021, as well as *in situ* temperature profiles, alongside modelled temperature profiles with internal waves removed, over the same 2-week period, across **(D)** Ile Anglaise, **(E)** Ile du Coin, and **(F)** Moresby. Note that no internal waves were detected in Ile du Coin, and therefore no model removing internal waves was run.

only 7% of the variance observed (n_g^2 = 0.07). The highest oxygen concentration was recorded in Ile Anglaise (277.06 μM on 30 September 2018). Daily DO cycles are observed across all three sites, but on average, the cycle in Ile du Coin was more pronounced, with values dipping below 165 μM around 6:00 a.m., compared to 180 and 185 μM in Ile Anglaise and Moresby, respectively (Figure 2).

Similarly, Ile du Coin also displayed the lowest pH values on average (7.91 ± 0.04), compared to Moresby (7.93 ± 0.02) and Ile Anglaise (7.96 ± 0.01) (Supplementary Figure S3). The lowest pH was also recorded in Ile du Coin, with a value of 7.78, compared to minimums of 7.92 and 7.86 in Ile Anglaise and Moresby, respectively. On average, pH was found to be significantly different across all three sites (ANOVA, F = 1,065.78, $p < 0.001$), and the site accounted for over 40% of the variance observed (n_g^2 = 0.42). Daily pH cycles were also, on average, more pronounced in the lagoon-facing reef (Figure 2). DO and pH were found to strongly correlate across all three sites throughout overlapping instrument deployments (Pearson's correlation; Ile Anglaise = 0.754, Moresby = 0.944, and Ile du Coin = 0.821, $p < 0.001$ for all three sites).

3.1.4 Comparison of *in situ* and *ex situ* measurements of temperature and wave heights

On average, sea surface temperatures retrieved using NOAA's CRW model were highly similar across all sites, with 28.75°C in Moresby and 28.72°C for both Ile du Coin and Ile Anglaise. The highest temperature was estimated to be in Ile du Coin (30.71°C), followed by Moresby, and then Ile Anglaise. Unlike *in situ* data, the lowest temperature was also estimated to occur in Ile du Coin (27.58°C). Comparing CRW SST values and *in situ* measurements shows that sSST does not capture internal wave events (Figure 4).

Wave heights measured using WaveWatch III (WWIII) were also found to be overestimated when compared to *in situ* using fast-sampling pressure sensors (Figure 4). From WWIII results, Ile du Coin and Moresby are located in the same grid cell; hence, the model gives no distinction of the wave height profiles at the two sites.

3.2 Total percentage cover and community composition of sessile communities across autonomous reef monitoring structures and sampling sites

A total of 27,144 identifications were made across the nine ARMS, of which 62.3% were assigned to sessile organisms across 22 benthic taxonomic groups, 6.2% were sediment, and 30.3% to noncolonised surfaces (no recruitment) (Supplementary Table S6). Some predation of sessile communities was observed, with 0.5% of counts identified as fish bite scars. Very few sessile organisms were unidentifiable, with an average of 1% of counts assigned as "unknown" across the three sites.

On average, the total percentage cover of live sessile organisms was the lowest in Ile du Coin (mean ± standard

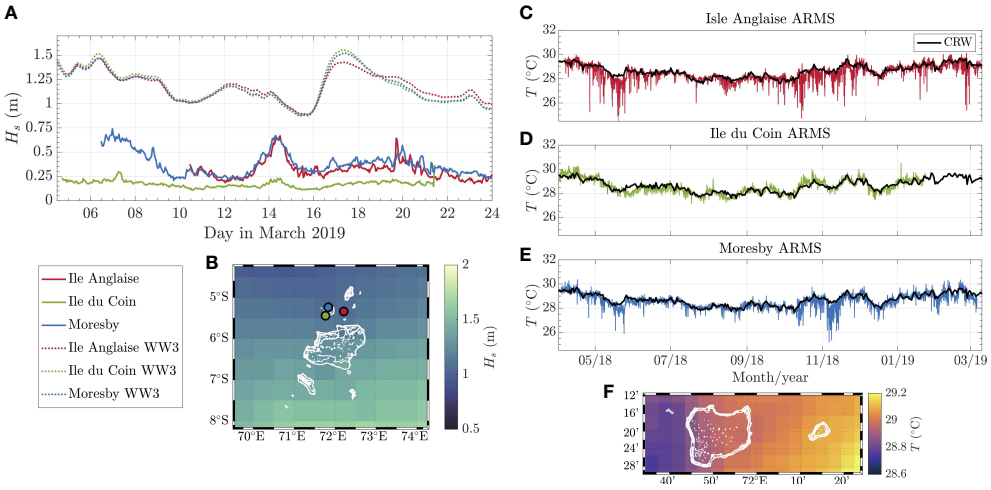

FIGURE 4
Comparison of *in situ* and *ex situ* data for wave heights (WaveWatch III model) and sea surface temperature (Coral Reef Watch (CRW) model) at each reef site. **(A)** Observed and estimated significant wave heights from the nearest WWIII cell during March 2019. **(B)** Visualisation of the WWIII resolution across the Chagos Archipelago marine-protected area (MPA), where one-coloured pixel represents a single value for the estimated wave height. **(C–E)** significant temperature values for individual reef sites (the black line represents CRW data, coloured lines represent *in situ* data). **(F)** Visualisation of the CRW resolution across the Peros Banos and Salomon atolls of the MPA, where one coloured pixel represents a single value for estimated temperature.

deviation, 61.12 ± 18.2%), compared to Ile Anglaise (73.34 ± 11.7%) or Moresby (73.16 ± 14.9%) reef sites. A quasibinomial GLM regression showed that both sites ($F = 14.26$, $p < 0.001$) and plate face ($F = 64.6$, $p < 0.001$) had a significant effect on overall live percentage cover across ARMS plates (full model output in Supplementary Table S8). *Post-hoc* Tukey's tests indicate that live percentage cover of sessile taxa was significantly higher on ARMS in Ile Anglaise ($p < 0.001$) and Moresby ($p < 0.001$) than at Ile du Coin. Live sessile percentage cover was also significantly higher on bottom plate faces (77% ± 1.23, $p < 0.001$) than on top plate faces (61% ± 2.02) across all sites. Sediment attached to or covering sessile organisms and plate surfaces were observed across all sampling sites despite efforts to shake these off (see Sec. 2. Materials and methods), with 9.4% of sessile counts in Ile du Coin assigned to this category compared to 4.5% in Moresby and 3.8% in Ile Anglaise.

Overall, sponges, soft-tube worms, and red macroalgae were the most abundant taxa groups in the lagoon-facing reef (Figure 5). On exposed reefs, bryozoans, sponges, and red and fleshy macroalgae were the most abundant, with red macroalgae in the highest abundance in Moresby and brown macroalgae in the highest abundance in Ile Anglaise (Figure 5).

The NMDS analysis showed the extent of dissimilarity between the top and bottom plate faces across sampling sites (Figure 6). Whilst the dispersion of data between the top and bottom plate face communities amongst triplicate ARMS was similar within Moresby and Ile Anglaise sites, a large difference was observed within Ile du Coin, with top plate face communities displaying a higher variability than bottom face communities (Figure 6).

The multivariate model indicated that site, plate face, and the interaction between both factors had a significant impact on the abundance of sessile taxonomic groups across ARMS (Table 1). Univariate regressions across groups showed that site choice has a significant impact on bryozoan, gastropod, and brown encrusting macroalgae abundances, whilst plate face had a significant effect on the abundance of calcified tube worms, soft tube worms, and colonial tunicates (Table 2). CCA, green encrusting, and red encrusting macroalgae abundance were also shown to be most abundant different across sites, but only when plate face is taken into account. Boxplots of these nine most taxa faces highlight these significant patterns, such as the contrast in red encrusting macroalgae abundance across the top and bottom plates in Ile du Coin in comparison to Ile Anglaise and Moresby and the dominance of brown encrusting macroalgae in Moresby (Figure 7).

3.3 Associations between environmental factors, habitat type, and benthic communities

dbRDA of *in situ* and *ex situ* temperature, pH, and DO, as well as flow velocity and wave heights, were all significant in

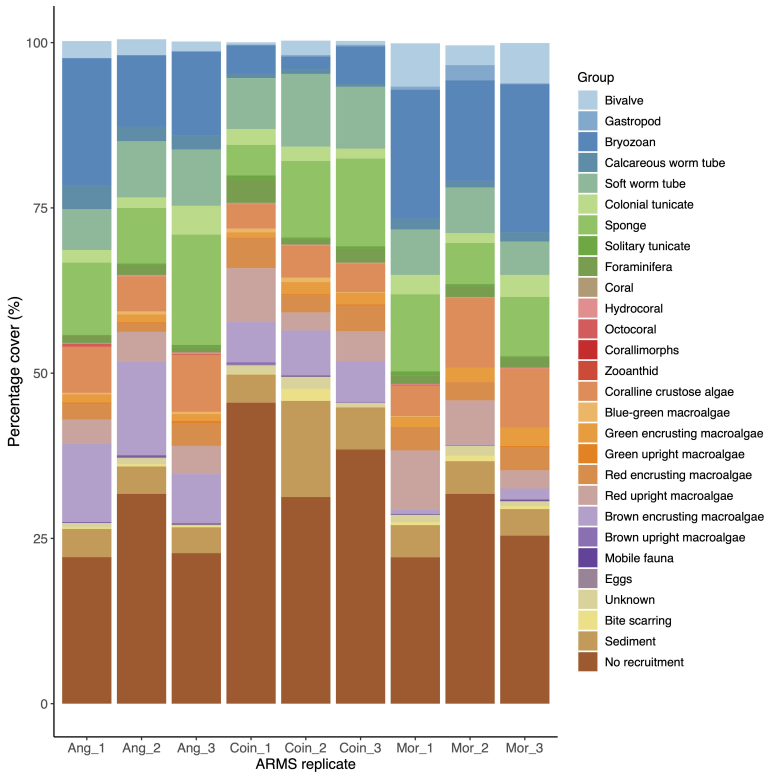

FIGURE 5
Stacked barplot displaying the percentage cover of sessile taxonomic groups, the percentage of counts assigned to non-sessile taxa as well as other identification groups, across replicates of autonomous reef monitoring structures (ARMS) from each sampling site (Ang, Ile Anglaise; Coin, Ile du Coin; Mor, Moresby).

explaining the same amount of variation observed in benthic communities across sites: *in situ* and *ex situ* temperature (permutation-based ANOVA, $F = 3.14$, p-value = 0.008, $R^2 = 0.31$, permutations = 999), pH, and DO ($F = 3.13$, p-value = 0.02, $R^2 = 0.31$), and flow velocity and wave heights ($F = 3.13$, p-value = 0.02, $R^2 = 0.31$) (Figure 8). Contrasting patterns of association were observed across the temperature model, with higher mean *ex situ* temperature associated with ARMS communities on ocean-facing reef Moresby ($F = 2.98$, p-value = 0.025) but higher *in situ* values associated with sheltered Ile du Coin ARMS communities ($F = 3.3$, p-value =0.017). Both mean pH values ($F = 2.74$, p-value = 0.035) and mean DO values ($F = 3.54$, p-value =0.018) were negatively associated with ARMS communities in the lagoon-facing reef. Mean flow velocity values were also negatively associated with Ile du Coin communities ($F = 3.28$, p-value = 0.025), whilst mean wave heights were positively associated with Moresby ARMS communities ($F = 3.00$, p-value = 0.023).

Our "indicspecies" analysis highlights correlations between average values of environmental parameters and taxa groups previously found to drive community dissimilarity between sampling sites and ARMS (Table 3). The percentage cover of CCA, colonial tunicates, green encrusting macroalgae, and bryozoans were observed to significantly correlate with sites presenting significantly higher DO values and lower temperature values. Bryozoan abundance also correlated significantly with higher PAR regimes observed across sites. The abundance of calcified tube worms found on both top and bottom plate face communities also significantly correlated with a lower *in situ* temperature regime and a higher DO regime. Brown encrusting macroalgae abundance on top plate face communities was observed to correlate with high pH and wave height regimes, as well as medium-flow velocities. Furthermore, the abundance of brown encrusting macroalgae across both plate faces correlated positively with lower PAR regimes. The abundance of red encrusting macroalgae on top and bottom plate face communities showed contrasting patterns of correlation with environmental parameters, with top plate abundances significantly correlating with medium wave and pH values and high flow velocities, whilst bottom plate abundances correlating with low DO and higher temperature profiles.

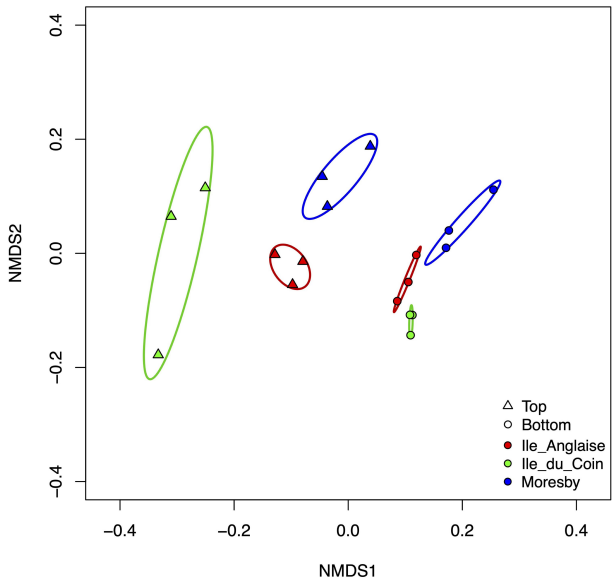

FIGURE 6
Non-metric multidimensional scaling (NMDS) ordination plots of autonomous reef monitoring structures (ARMS) communities on top or bottom plate faces across sampling sites, based on Bray–Curtis distances using fourth-root transformed count data and over two reduced dimensions (k = 2) (stress value = 0.106). Ellipses represent 95% confidence intervals fitted to the spatial ordination.

4 Discussion

4.1 *In situ* environmental profiles of the sampling sites

By measuring *in situ* physicochemical factors, we recover the environmental profile of three reefs over yearly, monthly, and daily time periods. Ocean-facing reefs (Moresby and Ile Anglaise) are characterised by higher and more variable flow regimes as well as higher wave heights compared to a lagoon-facing reef site. Flow regimes impact the accumulation of DO and particulate CO_2 in reef systems by interacting with sessile organisms' diffusive boundary layers (Finelli et al., 2006), and in part, can therefore, shape benthic metabolic rates. In our study, we observe significantly lower mean pH and DO values in a low-flow site when compared to two sites with high-flow regimes, as well as more variable average daily cycles of both parameters (Figure 2). Further work could investigate flow velocities across ARMS surfaces, as well as DO/pCO_2 fluxes, for example, using *in situ* incubation methods, as done by (Roth et al. 2019).

Internal wave events can reduce thermal stress on shallow reefs (Wyatt et al., 2020), but they also increase concentrations of nutrients (Reid et al., 2019) and fluxes of organic matter (Leichter et al., 1998) and decrease the risk of reef bleaching and mortality (Safaie et al., 2018). Within the Chagos Archipelago MPA, Sheppard (2008) previously recorded *in situ* temperature measurements across reef sites and found that internal wave events temporarily caused temperature drops of up to 7°C and that the effect increased with depth. We see similar dips in temperature across ocean-facing reefs in our study, with temperatures dropping up to ~5°C for short

TABLE 1 Summary of the statistical significance of a multivariate generalised linear models (GLMs) assessing the effect of site and plate face on the abundance of sessile groups.

Factors	Res.Df	Df.diff	Dev.	Pr(>Dev)
(Intercept)	17			
Site	15	2	133.4	**0.001*****
Plate face	14	1	229.4	**0.001*****
Site: plate face	12	2	149.4	**0.002****

Res.Df, residual degrees of freedom; Df.diff, difference in degrees of freedom; Dev, deviance; and Pr(>Dev), p-value. Full model output coefficients can be found in Supplementary Table S9.
Asterisks represent the level of significance of individual p-values (*when p<0.05, ** when p<0.01, *** when p<0.001).
Values in bold represent significant test p-values.

TABLE 2 Summary of the statistical significance of resampling-based univariate generalised linear models (GLMs) assessing the effect of site and plate face on the abundance of individual sessile groups.

Predictors	Bryozoan		Gastropods		Brown encrusting macroalgae	
	Dev	Pr(>Dev)	Dev	Pr(>Dev)	Dev	Pr(>Dev)
Site	17.62	**0.016***	17.95	**0.014***	19.66	**0.008****
Plate face	9.78	0.10	0.73	0.89	1.07	0.89
Site: plate face	2.40	0.96	2.25	0.96	7.14	0.56
	Colonial ascidians		**Soft-tube worms**		**Calcified tube worms**	
Site	0.14	1.00	0.25	0.99	12.1	0.12
Plate face	31.14	**0.001*****	62.38	**0.001*****	23.9	**0.001*****
Site: plate face	15.49	0.06	5.22	0.73	0.7	1.00
	Green encrusting macroalgae		**Red encrusting macroalgae**		**CCA**	
Site	1.99	0.91	2.59	0.85	1.79	0.92
Plate face	21.92	**0.002****	16.88	**0.003****	22.01	**0.002****
Site: plate face	17.18	**0.04***	20.30	**0.014***	20.86	**0.014***

Only taxa with significant values are listed. Dev, deviance; Pr(>Dev), p-value. Significant p-values are highlighted in bold (***p < 0.001; **p < 0.01; and *p < 0.05).

periods of time (Supplementary Figure S2). We see that sites where frequent internal waves occur (Ile Anglaise and Moresby) have significantly lower mean temperature values than a site where no internal waves are detected (Ile du Coin) (Figure 5). Indeed, internal waves contribute to the variability of temperature observed across our sites, even if they occur only 0.2%–0.42% of the time. Removing internal wave signals from our dataset and comparing edited temperature values across our sampling sites, result in an estimate that site choice alone accounts for 20 times more variance observed across temperature profiles than the same analysis of our dataset that does include internal waves. Our results suggest that measuring the temperature at short intervals is key for recovering accurate *in situ* benthic temperature profiles. Although not presented in the main body of this article, we also calculated degree-heating-days (DHD) across all three sites and show how internal waves reduce DHD by 8%–12% (Supplementary File S1). Whilst we did not investigate bleaching across ARMS communities in this study, we present methods and results of this additional analysis in the Supplementary material, as additional environmental context for future studies in this region (Supplementary File S1).

Satellite-derived SST is a popular metric for ecological studies of reef benthos (Carvalho et al., 2019; Floyd et al., 2020; Bosch et al., 2021), and with climate predictions indicating an increase in water temperatures globally (IPCC, 2022), it is important we obtain accurate temperature measurements when assessing or modelling the impact of heating on shallow reef cryptobenthic communities. Recent large-scale ARMS-based studies co-analysing benthic community diversity patterns and environmental parameters have used remote sensing data, including sSST and PAR (Carvalho et al., 2019; Pearman et al., 2020). Here, we show that *in situ* instrumentation is crucial for resolving patterns of local temperature and wave heights that cannot be detected using remote-sensing products. We find that NOAA's remote-sensing CRW model can overestimate and/or underestimate local temperatures across sites. For Ile du Coin, the sSST may underestimate actual sea surface conditions, and vice versa for the outer reef sites. This is because the mean SST provided by the CRW grid cell is 5 km × 5 km, covering both outer and inner reefs within the same grid, and hence does not offer data at the required resolution. Not detecting internal waves on reefs that experience them runs the risk of overestimating average temperature values and skewing estimates of heat stress on local communities. Temperature loggers are not expensive in comparison to other oceanographic instruments, and thus, we recommend that if budgets allow, temperature loggers should be deployed alongside ARMS. For wave heights, due to the coarse grid at the island scale, the WWIII model does not consider the sheltering effect of the archipelago (Pawka, 1983), and values were approximately five times larger than observed *in situ* wave heights. Our results show that the WWIII model is unable to recover individual wave profiles for each site, and therefore, we recommend that if resources allow, this model should not be used as a substitute for local, *in situ* measurements of wave exposure in the Chagos Archipelago MPA.

4.2 Percentage cover and diversity of autonomous reef monitoring structures sessile communities

Our image analysis recovers a diverse community of benthic invertebrate and algal groups after 1 year. Other studies have investigated the sessile benthic community composition and condition of exposed reef surfaces across the Chagos

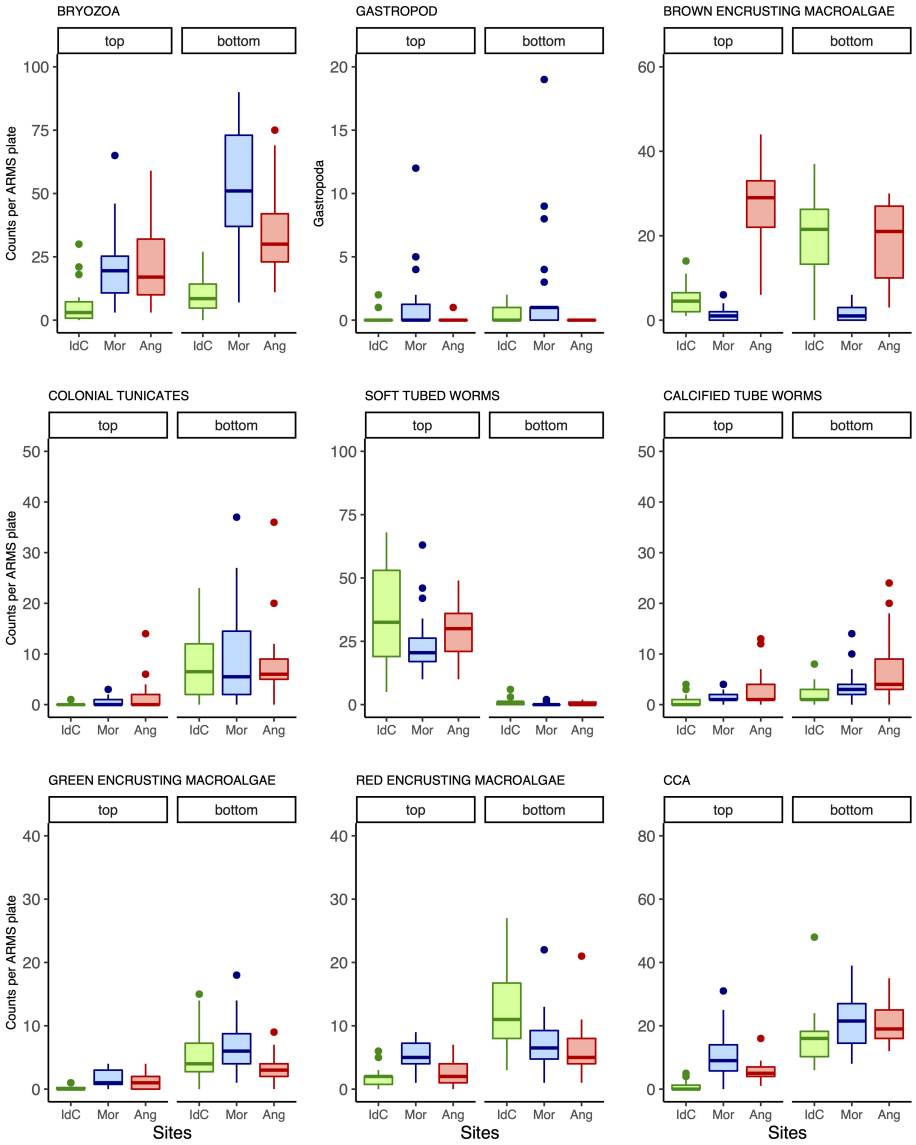

FIGURE 7
Boxplots comparing the counts of nine taxonomic groups were found to have significantly different abundances across autonomous reef monitoring structures (ARMS) plate face and/or across sampling sites (IdC, Ile du Coin; Mor, Moresby; and Ang, Ile Anglaise).

Archipelago MPA (Head et al., 2019; Lange et al., 2021; Pilly et al., 2022), but none have previously investigated sessile cryptobenthic communities in this region. We find that sponges, fleshy and calcareous macroalgae, bryozoans, and annelid worms dominated recruitment surfaces, whilst colonial ascidians, molluscs, colonial ascidians, tunicates, and large foraminifera were less frequently observed.

Our findings show that the site also has a significant effect on ARMS community composition. Whilst almost all taxonomic groups are observed across all three sites (except for octocorals), and triplicate ARMS devices harbour highly similar communities within sites, overall community composition between reefs significantly differs. Image analysis has been shown to effectively recover the benthic profile of different sites using triplicate ARMS devices (David et al., 2019), and previous genetic analyses found that differences in sampling site and region shape the cryptobenthic composition and diversity on ARMS (Pearman et al., 2020). Here, by analysing 15 plate faces per device and following NOAA's CREP program's identification groupings, we demonstrate that ARMS photoanalysis alone can discriminate amongst reef sites within the same region, as well as between sites with similar local environmental conditions. The analysis of 225 points across 15 images per ARMS was feasible here due to the restricted number

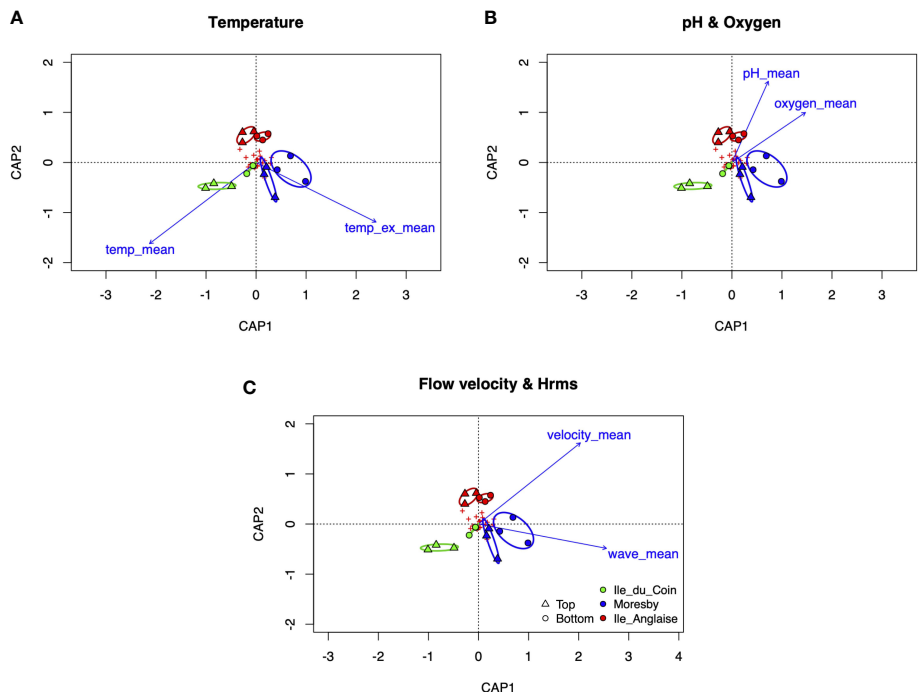

FIGURE 8
Distance-based redundancy analysis (db-RDA) ordinations of top or bottom plate face benthic communities across sites, based on Bray–Curtis distances using fourth-root transformed count data, factored with mean **(A)** *in situ* (temp_mean) and *ex situ* temperatures (temp_ex_mean), **(B)** pH and oxygen, and **(C)** flow velocity and wave heights. Ellipses represent 95% confidence intervals fitted to the spatial ordination. Red crosses highlight the positioning of benthic groups amongst the ordination.

of sampling sites, but future studies could employ automated annotation tools, such as CoralNet's latest deep-learning engine, to increase coverage and decrease analysis time (Beijbom et al., 2015; Chen et al., 2021).

We also see a strong and significant effect of plate face on the composition of ARMS benthic communities. Indeed, we observe a significantly lower percentage cover and significantly different assemblages of taxonomic groups on the top faces of ARMS plates than on the bottom faces, across all three sites. Our results show that several filter-feeding invertebrates and macroalgal taxa are significantly more abundant on the underside of ARMS plates, whilst only soft-tube annelids are found in higher abundance on top plate faces (Table 2). Similar patterns of community composition have been observed under sheeting coral colonies (Jackson and Winston, 1982), within reef cavities (Scheffers et al., 2010; Kornder et al., 2021), on artificial recruitment tiles (Higgins et al., 2019; Mallela et al., 2017), as well as by David et al. (2019) on the underside of ARMS plates from the Red Sea. We find that together, plate face and site choice significantly contribute to differences observed in the abundance of CCA, fleshy red encrusting algae and green encrusting algae across sampled reefs. Whilst the percentage cover of fleshy macroalgae has been estimated to be between 1% and 4% across shallow reefs of the Chagos Archipelago (Head et al., 2019; Lange et al., 2021), they represent around a third of benthic communities across ARMS devices in this study. Unlike some cryptobenthic invertebrates (e.g., bryozoan, ascidian, and encrusting sponges), macroalgae are often included in reef biomonitoring protocols and surveys. Encrusting macroalgae are commonly found within cryptic reef cavities but often form a minor part of organism biomass within cryptobenthic communities (Kornder et al., 2021). Our findings highlight how traditional benthic surveys, where only exposed surfaces are analysed, could underestimate the true percentage cover of key phototrophic groups. However, further comparisons between the cryptobenthic communities found on ARMS and those on nearby cryptic surfaces and cavities are now needed to determine if ARMS plates overestimate the percentage cover of any taxa. Nevertheless, based on our findings, we recommend that future image-based studies of ARMS from tropical coral reefs investigate top and bottom plate communities independently.

The presence of sand and sediment on top plates likely impacts the percentage cover and community composition across the top and bottom surfaces of ARMS devices. Sediment loading on reef surfaces has been shown to negatively affect the recruitment of stony coral, sponges, tunicates, and CCA (Fabricius and De'ath, 2001; Babcock and Smith, 2002; Maldonado et al., 2008) and can have mixed impacts on fleshy macroalgae recruitment by either inhibiting or abrading zygote attachment (Gao et al., 2019) or conversely by reducing fish and urchin herbivory (Tebbett et al., 2018; Kriegisch

TABLE 3 Results of point biserial correlation analyses of benthic groups with mean environmental parameter values, across either top or bottom plate communities.

Environmental parameter	State	Taxonomic group	*r*	*p*-value
Flow/wave height	High	Red encrusting macroalgae (T)	0.936	0.377*
	Medium	Brown encrusting macroalgae (T)	0.87	0.035*
In situ temperature	High	Soft worm tube (T)	0.765	0.045*
		Red encrusting macroalgae (B)	0.778	0.025*
	Low	CCA (T)	0.901	0.012*
		Calcified worm tube (T + B)	0.879 (T)	0.012* (T)
			0.811 (B)	0.012* (B)
		Green encrusting macroalgae (T)	0.722	0.012*
		Tunicate colonial (T)	0.715	0.025*
		Bryozoan (B)	0.878	0.012*
pH	Medium	Red encrusting macroalgae (T)	0.936	0.036*
	High	Brown encrusting macroalgae (T)	0.87	0.036*
DO	High	CCA (T)	0.901	0.014*
		Calcified worm tube (T + B)	0.879 (T)	0.014* (T)
			0.811 (B)	0.013* (B)
		Bryozoan (T + B)	0.837 (T)	0.014* (T)
			0.878 (B)	0.013* (B)
		Green encrusting macroalgae (T)	0.722	0.014*
		Tunicate colonial (T)	0.715	0.026*
	Low	Red encrusting macroalgae (B)	0.778	0.025*
PAR	High	CCA (T)	0.755	0.033*
		Red encrusting macroalgae (T)	0.953	0.011*
		Bryozoan (B)	0.832	0.022*
	Low	Brown encrusting macroalgae (T + B)	0.903 (T)	0.036* (T)
			0.870 (B)	0.012* (B)

Only taxa with significant correlations ($p < 0.05$) are displayed, along with their correlation coefficient (r). Furthermore, only taxa whose abundance was previously found to be significantly impacted by site and plate face with multivariate generalised linear models (GLMs) are presented in this table (see Sec. 2. Materials and methods). CCA, crustose coralline algae; DO, dissolved oxygen; and PAR, photosynthetically active radiation.
Asterisks represent the level of significance of individual p-values (*when $p<0.05$, ** when $p<0.01$, *** when $p<0.001$).

et al., 2019). We did not record actual sedimentation rates in this study but recommend pilot studies now be conducted on the extent of sedimentation on ARMS, for example, by using traps (Storlazzi et al., 2011) to record accumulation rates throughout unit deployments.

4.3 Associations between cryptobenthic communities and environmental parameters

We find that some of the variations in ARMS cryptobenthic communities observed across our three study sites can be explained by differences in mean *in situ* or *ex situ* temperature, pH, DO, flow velocities, and wave heights. Previous ARMS-based studies found that SST, PAR, pH, and surrounding coral cover are important variables in shaping the taxonomic diversity of sessile, mobile, or microbial communities across geographic regions (Pearman et al., 2019; Pearman et al., 2020). We recognise that benthic assemblages can show non-linear responses to changes in abiotic factors in reef ecosystems (Gove et al., 2015) and that our dbRDA analysis only represents a facet of biophysical interactions between benthic communities and environmental parameters. In part, this is due to our small number of site replicates and the fact that mean values offer limited information on long-term datasets. Nevertheless, our results support the need for *in situ* physicochemical measurements rather than remote sensing. For example, the temperature dbRDA displays contrasting trends, with increasing mean *in situ* temperature values associated only with Ile du Coin communities but *ex situ* values significantly associated only with Moresby communities (Figure 8). This finding highlights the risk that *in situ* biophysical relationships could be misinterpreted when using satellite-derived SST for the study of cryptobenthic communities across reefs in close geographical proximity.

The abundance of some cryptobenthic taxa on ARMS devices significantly correlates with different regimes of temperature, pH, PAR, oxygen, flow velocity, and wave heights observed across our sampling sites (Table 3). For some groups (e.g., red fleshy macroalgae), we find that abundances on top and bottom plate face communities significantly correlate with a

different set of environmental drivers, whilst for others (e.g., calcareous worms and bryozoans), both top and bottom plate face abundances correlate with the same environmental regimes.

We find that encrusting macroalgal groups correlate differently with *in situ* environmental regimes identified across our sampling sites. Top-plate CCA abundance correlates with lower *in situ* temperature profiles, but the opposite is observed for fleshy red encrusting macroalgae abundance on the underside of ARMS plates (Table 3). On top plate communities, we see that red and brown macroalgal abundance correlates with medium/high flow (10–12 cm/s) and wave height regimes (0.27–0.34 m), as well as medium/high pH profiles (7.93–7.96). Growth responses of fleshy marine macroalgae to water flow rates can be based on species-specific physiological adaptations (Ho and Carpenter, 2017), and water flow can increase photosynthetic rates, and therefore growth, up to a point (Stewart and Carpenter, 2003). Macroalgae of different forms can interact both positively or negatively, through competition for resources (Fong and Paul, 2011) or by protecting one another from herbivory and sediment loading (Bittick et al., 2010; Sura et al., 2019), and competition may play a role in shaping macroalgal abundances observed between reef sites in this study.

CCA form a major component of benthic calcifiers on reefs but have shown to fare worse than their non-calcifying counterparts under higher temperatures and lower pH conditions (Porzio et al., 2011; Zweng et al., 2018; Diaz-Pulido and Barrón, 2020), a worrying trend for the future of accreting reefs as oceans continue to warm and acidify. Our environmental analysis shows that average pH values differ significantly between sites, and whilst the pH at the sheltered site (Ile du Coin) was found to be at 7.91 on average; the large diel variations observed *in situ* resulted in minimum values at or below 7.85 (Figure 2; Supplementary Figure S3). These minimum pH values, alongside higher temperatures, may not be more conducive for the growth of CCA at this site, as co-occurring low pH and high-temperature conditions can reduce calcification and productivity rates (Anthony et al., 2008; Diaz-Pulido et al., 2012). To further investigate the relationship between *in situ* temperature, DO, and pH and the abundance of both calcifying and encrusting macroalgae, net community calcification (NCC) and net community productivity (NCP) could be calculated. Longer deployments of SeapHOx/SeaFET loggers, matching those of temperature loggers, would also be needed to identify the extent of time during which ARMS communities experience acidifying conditions.

We find that increases in the abundance of other calcifying groups, bryozoans, and calcareous tube worms, also significantly correlate with lower *in situ* temperature and higher DO regimes (Table 3). Differences in thermal tolerance have been shown in bryozoans across marine habitats (see review by Lombardi et al., 2020), but co-occurring low pH and high temperatures can negatively affect bryozoan cover by reducing growth and calcification rates as well as increasing the dissolution of dead colonies (Rodolfo-Metalpa et al., 2010). Calcareous serpulids have been shown to thrive on reefs experiencing regular cooling (Leichter et al., 1998). However, co-occurring low-oxygen and high-temperature conditions can be unfavourable for the growth rate of calcifying reef organisms in general (Nelson and Altieri, 2019). Whilst frequent internal waves at Ile Anglaise and Moresby likely provide a conducive environment for calcareous worms and bryozoan growth through regular cooling, these events may also benefit these groups through the regular upwelling of prey plankton and nutrients (Leichter et al., 1998), as well as a mechanism for increased larval dispersal (Fernández-Aldecoa et al., 2019).

4.4 Study limitations

We recognise there are several potential limitations to our study's methodologies. Firstly, we made observations of cryptobenthic groups at a high taxonomic level, limiting our ability to look at diversity patterns across ARMS and sites. Restricted time in the field and limited resources for the identification of sessile cryptobenthic species available for this region meant we were unable to classify organisms to lower levels. Furthermore, our 2D photography of ARMS surface cover likely neglects the 3D structure of cryptobenthic reef communities (Kornder et al., 2021), and since photographs were taken from a top-down perspective, organisms with the ability to grow over others are more likely to have been visible and therefore recorded. Whilst we find that not all available ARMS recruitment surface was covered by live sessile organisms, we observed that recruitment cover was denser on the outer edges of ARMS plates, which are usually composed of both overlapping encrusting and upright macroalgae. Future ARMS studies could employ fluorescence photography, as shown in Steyaert et al. (2022), to improve estimates of the percentage cover of encrusting organisms, such as CCA and juvenile hard corals, using group-specific wavelengths.

Secondly, the number of site replicates ($n = 3$) in our study limits our ability to simultaneously model the relationship between multiple environmental parameters and community composition. We explore correlations between taxa abundances and *in situ* environmental profiles but cannot perform regression-based models integrating all parameters simultaneously. Increasing the number of sites and merging this dataset with other ARMS studies across the Indian Ocean could provide enough sampling replicates, as done by Pearman et al. (2020).

Thirdly, whilst we have long-term data on environmental parameters over a full year, we analyse cryptobenthic communities only at the end of these 12 months. Such is the nature of current ARMS studies that once collected, sessile communities on each unit are subsampled and scraped off. However, pilot studies could explore the potential of ARMS to act as long-term biomonitoring stations, where plates could be photographed and then re-assembled and re-deployed.

5 Conclusion

The need for continuous and comprehensive monitoring of both benthic communities and environmental parameters on coral reefs is crucial in the face of increasing climate change impacts (Koldewey et al., 2021). Whilst the degradation of coral reef habitats is set to reduce (Brandl et al., 2020) or alter (Kubicek et al., 2019) diversity over the coming decades, relatively few studies have been conducted on the functional or taxonomic diversity of sessile invertebrates or macroalgae on tropical reefs in comparison with hard corals and fish (Brandl et al., 2019). Fewer studies have co-analysed *in situ* environmental parameters and the biodiversity of cryptic reef spaces (but see Scheffers et al., 2010; Kornder et al., 2021). By analysing large and detailed datasets of benthic communities and environmental parameters from three tropical reef sites, we identify subtle but significant differences in the abundance and composition of cryptobenthic taxa and the environmental profile that they experience, after just 1 year. Our study provides an example of how *in situ* environmental parameters can be integrated with image-analysis data for future ARMS-based monitoring efforts and is the first step in this endeavour for the reefs of the Chagos Archipelago.

Data availability statement

Benthic abundance data from the analysis of Autonomous Reef Monitoring Structure (ARMS) images presented in this study is included in the article/Supplementary Material. Further inquiries regarding this dataset, and any enquiries regarding environmental/physical data presented in this study, can be directed to the corresponding author.

Author contributions

MS, AK, ML, CH, RB, and DM collected the data. MS, AK, ML, and PW analysed the data. All authors made substantial contributions to the discussion of the content, the writing, and the editing of the manuscript. All authors contributed to the article and approved the submitted version.

Funding

This work was funded by the Bertarelli Foundation as part of the Bertarelli Programme in Marine Science.

Acknowledgments

The authors would like to thank April Burt (University of Oxford) for her assistance in the deployment of autonomous reef monitoring structures for the purpose of this study.

Conflict of interest

The authors declare that the research was conducted in the absence of any commercial or financial relationships that could be construed as a potential conflict of interest.

Publisher's note

Supplementary material

The Supplementary Material for this article can be found online at: https://www.frontiersin.org/articles/10.3389/fmars.2022.932375/full#supplementary-material

References

Al-Rshaidat, M. M., Snider, A., Rosebraugh, S., Devine, A. M., Devine, T. D., Plaisance, L., et al. (2016). Deep COI sequencing of standardized benthic samples unveils overlooked diversity of Jordanian coral reefs in the northern red Sea. *Genome* 59, 724–737. doi: 10.1139/gen-2015-0208

Anthony, K. R., Kline, D. I., Diaz-Pulido, G., Dove, S., and Hoegh-Guldberg, O. (2008). Ocean acidification causes bleaching and productivity loss in coral reef builders. *Proc. Natl. Acad. Sci. U. S. A.* 105, 17442–17446. doi: 10.1073/pnas.0804478105

Appeltans, W., Ahyong, S. T., Anderson, G., Angel, M. V., Artois, T., Bailly, N., et al. (2012). The magnitude of global marine species diversity. *Curr. Biol.* 22, 2189–2202. doi: 10.1016/j.cub.2012.09.036

Babcock, R., and Smith, L. (2002). "Effects of sedimentation on coral settlement and survivorship," in *Proceedings of the 9th International Coral Reef Symposium*, Bali, 23-27 October 2000, Vol. 1. 245–248.

Beijbom, O., Edmunds, P. J., Roelfsema, C., Smith, J., Kline, D. I., Neal, B. P., et al. (2015). Towards automated annotation of benthic survey images: Variability of human experts and operational modes of automation. *PloS One* 10, e0130312. doi: 10.1371/journal.pone.0130312

Bell, J. J., Bennett, H. M., Rovellini, A., and Webster, N. S. (2018). Sponges to be winners under near-future climate scenarios. *Bioscience.* 68, 955–968. doi: 10.1093/biosci/biy142

Bittick, S. J., Bilotti, N. D., Peterson, H. A., and Stewart, H. L. (2010). Turbinaria ornata as an herbivory refuge for associate algae. *Mar. Biol.* 157, 317–323. doi: 10.1007/s00227-009-1319-6

Bosch, N. E., Wernberg, T., Langlois, T. J., Smale, D. A., Moore, P. J., Franco, J. N., et al. (2021). Niche and neutral assembly mechanisms contribute to latitudinal diversity gradients in reef fishes. *J. Biogeogr.* 48, 2683–2698. doi: 10.1111/jbi.14237

Brandl, S. J., Johansen, J. L., Casey, J. M., Tornabene, L., Morais, R. A., and Burt, J. A. (2020). Extreme environmental conditions reduce coral reef fish biodiversity and productivity. *Nat. Commun.* 11, 1–14. doi: 10.1038/s41467-020-17731-2

Brandl, S. J., Rasher, D. B., Côté, I. M., Casey, J. M., Darling, E. S., Lefcheck, J. S., et al. (2019). Coral reef ecosystem functioning: eight core processes and the role of biodiversity. *Front. Ecol. Environ.* 17, 445–454. doi: 10.1002/fee.2088

Cáceres, M. D., and Legendre, P. (2009). Associations between species and groups of sites: indices and statistical inference. *Ecology* 90, 3566–3574. doi: 10.1890/08-1823.1

Cahyani, N. K. D. (2021). *Delineating macro and micro marine biodiversity in the coral triangle using autonomous reef monitoring structures and DNA metabarcoding. [dissertation]* (Los Angeles, USA: University of California).

Carvalho, S., Aylagas, E., Villalobos, R., Kattan, Y., Berumen, M., and Pearman, J. K. (2019). Beyond the visual: using metabarcoding to characterize the hidden reef cryptobiome. *Proc. R. Soc B: Biol. Sci.* 286, 20182697. doi: 10.1098/rspb.2018.2697

Chen, Q., Beijbom, O., Chan, S., Bouwmeester, J., and Kriegman, D. (2021). *A new deep learning engine for CoralNet.* 3693–3702. doi. 10.1109/ICCVW54120.2021.00412

Colin, P. L., and Johnston, T. M. (2020). Measuring temperature in coral reef environments: Experience, lessons, and results from Palau. *J. Mar. Sci. Eng.* 8, 680. doi: 10.3390/jmse8090680

Cornwall, C., Comeau, S., DeCarlo, T., Larcombe, E., Moore, B., Giltrow, K., et al. (2020). A coralline alga gains tolerance to ocean acidification over multiple generations of exposure. *Nat. Clim. Change.* 10, 143–146. doi: 10.1038/s41558-019-0681-8

David, R., Uyarra, M. C., Carvalho, S., Anlauf, H., Borja, A., Cahill, A. E., et al. (2019). Lessons from photo analyses of autonomous reef monitoring structures as tools to detect (bio-) geographical, spatial, and environmental effects. *Mar. pollut. Bull.* 141, 420–429. doi: 10.1016/j.marpolbul.2019.02.066

Davis, K. L., Colefax, A. P., Tucker, J. P., Kelaher, B. P., and Santos, I. R. (2021). Global coral reef ecosystems exhibit declining calcification and increasing primary productivity. *Commun. Earth Environ.* 2, 1–10. doi: 10.1038/s43247-021-00168-w

DeCarlo, T. M., Carvalho, S., Gajdzik, L., Hardenstine, R. S., Tanabe, L. K., Villalobos, R., et al. (2021). Patterns, drivers, and ecological implications of upwelling in coral reef habitats of the southern red Sea. *J. Geophys. Res.* 126, e2020JC016493. doi: 10.1029/2020JC016493

de Goeij, J. M., and Van Duyl, F. C. (2007). Coral cavities are sinks of dissolved organic carbon (DOC). *Limnol. Oceanogr.* 52, 2608–2617. doi: 10.4319/lo.2007.52.6.2608

Diaz-Pulido, G., Anthony, K. R., Kline, D. I., Dove, S., and Hoegh-Guldberg, O. (2012). Interactions between ocean acidification and warming on the mortality and dissolution of coralline algae 1. *J. Phycol.* 48, 32–39. doi: 10.1111/j.1529-8817.2011.01084.x

Diaz-Pulido, G., and Barrón, C. (2020). CO2 enrichment stimulates dissolved organic carbon release in coral reef macroalgae. *J. Phycol.* 56, 1039–1052. doi: 10.1111/jpy.13002

Fabricius, K., and De'ath, G. (2001). Environmental factors associated with the spatial distribution of crustose coralline algae on the great barrier reef. *Coral Reefs* 19, 303–309. doi: 10.1007/s003380000120

Fernández-Aldecoa, R. G., Ladah, L. B., Morgan, S. G., Dibble, C. D., Solana-Arellano, E., and Filonov, A. (2019). Delivery of zooplankton to the surf zone during strong internal tidal forcing and onshore winds in Baja California. *Mar. Ecol. Prog. Ser.* 625, 15–26. doi: 10.3354/meps13034

Finelli, C. M., Helmuth, B. S., Pentcheff, N. D., and Wethey, D. S. (2006). Water flow influences oxygen transport and photosynthetic efficiency in corals. *Coral Reefs.* 25, 47–57. doi: 10.1007/s00338-005-0055-8

Floyd, M., Mizuyama, M., Obuchi, M., Sommer, B., Miller, M. G., Kawamura, I., et al. (2020). Functional diversity of reef molluscs along a tropical-to-temperate gradient. *Coral Reefs* 39, 1361–1376. doi: 10.1007/s00338-020-01970-2

Fong, P., and Paul, V. J. (2011). "Coral reef algae," in *Coral reefs: An ecosystem in transition* (Dordrecht: Springer), 241–272.

Gao, X., Lee, J. R., Park, S. K., Kim, N. G., and Choi, H. G. (2019). Detrimental effects of sediment on attachment, survival and growth of the brown alga *Sargassum thunbergii* in early life stages. *Phycol. Res.* 67, 77–81. doi: 10.1111/pre.12347

Gelman, A., and Hill, J. (2006). *Data analysis using regression and multilevel/hierarchical models* (Cambridge: Cambridge University Press).

Gove, J. M., Williams, G. J., McManus, M. A., Clark, S. J., Ehses, J. S., and Wedding, L. M. (2015). Coral reef benthic regimes exhibit non-linear threshold responses to natural physical drivers. *Mar. Ecol. Prog. Ser.* 522, 33–48. doi: 10.3354/meps11118

Hays, G. C., Koldewey, H. J., Andrzejaczek, S., Attrill, M. J., Barley, S., Bayley, D. T., et al. (2020). A review of a decade of lessons from one of the world's largest MPAs: conservation gains and key challenges. *Mar. Biol.* 167, 1–22. doi: 10.1007/s00227-020-03776-w

Head, C. E., Bayley, D. T., Rowlands, G., Roche, R. C., Tickler, D. M., Rogers, A. D., et al. (2019). Coral bleaching impacts from back-to-back 2015–2016 thermal anomalies in the remote central Indian ocean. *Coral Reefs* 38, 605–618. doi: 10.1007/s00338-019-01821-9

Head, C. E., Bonsall, M. B., Jenkins, T. L., Koldewey, H., Pratchett, M. S., Taylor, M. L., et al. (2018). Exceptional biodiversity of the cryptofaunal decapods in the chagos archipelago, central Indian ocean. *Mar. pollut. Bull.* 135, 636–647. doi: 10.1016/j.marpolbul.2018.07.063

Higgins, E., Scheibling, R. E., Desilets, K. M., and Metaxas, A. (2019). Benthic community succession on artificial and natural coral reefs in the northern gulf of aqaba, red Sea. *PloS One* 14, e0212842. doi: 10.1371/journal.pone.0212842

Ho, M., and Carpenter, R. C. (2017). Differential growth responses to water flow and reduced pH in tropical marine macroalgae. *J. Exp. Mar. Biol. Ecol.* 491, 58–65. doi: 10.1016/j.jembe.2017.03.009

Ho, M., McBroom, J., Bergstrom, E., and Diaz-Pulido, G. (2021). Physiological responses to temperature and ocean acidification in tropical fleshy macroalgae with varying affinities for inorganic carbon. *ICES J. Mar. Sci.* 78, 89–100. doi: 10.1093/icesjms/fsaa195

Hu, Y., Beggs, H., and Wang, X. H. (2021). Intercomparison of highresolution SST climatologies over the Australian region. *J. Geophys. Res. Oceans* (126), e2021JC017221. doi: 10.1029/2021JC017221

IPCC (2022). "Climate change 2022: Mitigation of climate change," in *Contribution of working group III to the sixth assessment report of the intergovernmental panel on climate change* (Cambridge: Cambridge University Press).

Jackson, J., and Winston, J. E. (1982). Ecology of cryptic coral reef communities. i. distribution and abundance of major groups of encrusting organisms. *J. Exp. Mar. Biol. Ecol.* 57, 135–147. doi: 10.1016/0022-0981(82)90188-5

Klumpp, D. W., McKinnon, A. D., and Mundy, C. N. (1988). Motile cryptofauna of a coral reef: Abundance, distribution and trophic potential. *Mar. Ecol. Prog. Ser.* 45, 95–108. doi: 10.3354/meps045095

Koldewey, H., Atchison-Balmond, N., Graham, N., Jones, R., Perry, C., Sheppard, C., et al. (2021). Key climate change effects on the coastal and marine environment around the Indian ocean UK overseas territories. *MCCIP Sci. Rev.* 2021, 2.

Kornder, N. A., Cappelletto, J., Mueller, B., Zalm, M. J., Martinez, S. J., Vermeij, M. J., et al. (2021). Implications of 2D versus 3D surveys to measure the abundance and composition of benthic coral reef communities. *Coral Reefs*, 1–17. doi: 10.1007/s00338-021-02118-6

Kriegisch, N., Reeves, S. E., Johnson, C. R., and Ling, S. D. (2019). Top-down sea urchin overgrazing overwhelms bottom-up stimulation of kelp beds despite sediment enhancement. *J. Exp. Mar. Biol. Ecol.* 514, 48–58. doi: 10.1016/j.jembe.2019.03.012

Kroeker, K., Micheli, F., and Gambi, M. (2013). Ocean acidification causes ecosystem shifts *via* altered competitive interactions. *Nat. Clim. Change.* 3, 156–159. doi: 10.1038/nclimate1680

Kubicek, A., Breckling, B., Hoegh-Guldberg, O., and Reuter, H. (2019). Climate change drives trait-shifts in coral reef communities. *Sci. Rep.* 9, 1–10. doi: 10.1038/s41598-019-38962-4

Lange, I. D., and Perry, C. T. (2019). Bleaching impacts on carbonate production in the chagos archipelago: influence of functional coral groups on carbonate budget trajectories. *Coral Reefs* 38, 619–624. doi: 10.1007/s00338-019-01784-x

Lange, I. D., Benkwitt, C. E., McDevitt-Irwin, J. M., Tietjen, K. L., Taylor, B., Chinkin, M, et al. (2021). Wave exposure shapes reef community composition and recovery trajectories at a remote coral atoll. *Coral Reefs* 40, 1819–1829

Leichter, J. J., Shellenbarger, G., Genovese, S. J., and Wing, S. R. (1998). Breaking internal waves on a Florida (USA) coral reef: a plankton pump at work? *Mar. Ecol. Prog. Ser.* 166, 83–97. doi: 10.3354/meps166083

Leray, M., and Knowlton, N. (2015). DNA Barcoding and metabarcoding reveal patterns of diversity in cryptic benthic communities. *Proc. Natl. Acad. Sci. U. S. A.* 112, 2076–2081. doi: 10.1073/pnas.1424997112

Leray, M., and Knowlton, N. (2016). Censusing marine eukaryotic diversity in the twenty-first century. *Philos. Trans. R. Soc B: Biol. Sci.* 371, 20150331. doi: 10.1098/rstb.2015.0331

Lesser, M. P., Slattery, M., and Leichter, J. J. (2009). Ecology of mesophotic coral reefs. *J. Exp. Mar. Biol. Ecol.* 375, 1–8. doi: 10.1016/j.jembe.2009.05.009

Liu, G., Matrosova, L. E., Penland, C., Gledhill, D. K., Eakin, C. M., Webb, R. S., et al. (2008). NOAA Coral reef watch coral bleaching outlook system. (Ft. Lauderdale, Florida: Proceedings of the 11th International Coral Reef Symposium) 951–955.

Lombardi, C., Taylor, P. D., and Cocito, S. (2020). "Bryozoans: The forgotten bioconstructors," in *Perspectives on the marine animal forests of the world* (Springer), 193–217.

Lopes, A. R., Faleiro, F., Rosa, I. C., Pimentel, M. S., Trubenbach, K., Repolho, T., et al. (2018). Physiological resilience of a temperate soft coral to ocean warming and acidification. *Cell Stress Chaperones.* 23, 1093–1100. doi: 10.1007/s12192-018-0919-9

Maldonado, M., Giraud, K., and Carmona, C. (2008). Effects of sediment on the survival of asexually produced sponge recruits. *Mar. Biol.* 154, 631–641. doi: 10.1007/s00227-008-0956-5

Mallela, J., Milne, B. C., and Martinez-Escobar, D. (2017). A comparison of epibenthic reef communities settling on commonly used experimental substrates: PVC versus ceramic tiles. *J. Exp. Mar. Biol. Ecol.* 486, 290–295. doi: 10.1016/j.jembe.2016.10.028

Meesters, E., Knijn, R., Willemsen, P., Pennartz, R., and Roebers, G. (1991). Sub-Rubble communities of curaçao and bonaire coral reefs. *Coral Reefs* 10, 189–197. doi: 10.1007/BF00336773

Nelson, H. R., and Altieri, A. H. (2019). Oxygen: the universal currency on coral reefs. *Coral Reefs* 38, 177–198. doi: 10.1007/s00338-019-01765-0

Nichols, P. K., Timmers, M., and Marko, P. B. (2022). Hide 'n seq: Direct versus indirect metabarcoding of coral reef cryptic communities. *Environ. DNA.* 4, 93–107. doi: 10.1002/edn3.203

Obst, M., Exter, K., Allcock, A. L., Arvanitidis, C., Axberg, A., Bustamante, M., et al. (2020). A marine biodiversity observation network for genetic monitoring of hard-bottom communities (ARMS-MBON). *Front. Mar. Sci.* 7, 572680. doi: 10.3389/fmars.2020.572680

Oksanen, J., Blanchet, F. G., Kindt, R., Legendre, P., Minchin, P. R., O'hara, R. B., et al. (2013). *Package 'vegan'. community ecology package, version 2.* 1–295.

Pan, X., Wong, G. T., DeCarlo, T. M., Tai, J., and Cohen, A. L. (2017). Validation of the remotely sensed nighttime sea surface temperature in the shallow waters at the dongsha atoll. *Terr. Atmos. Ocean. Sci.* 28, 517–524. doi: 10.3319/TAO.2017.03.30.01

Pawka, S. S. (1983). Island shadows in wave directional spectra. *J. Geophys. Res. Oceans.* 88, 2579–2591. doi: 10.1029/JC088iC04p02579

Pawlik, J. R., and McMurray, S. E. (2020). The emerging ecological and biogeochemical importance of sponges on coral reefs. *Ann. Rev. Mar. Sci.* 1, 315–337. doi: 10.1146/annurev-marine-010419-010807

Pearman, J. K., Aylagas, E., Voolstra, C. R., Anlauf, H., Villalobos, R., and Carvalho, S. (2019). Disentangling the complex microbial community of coral reefs using standardized autonomous reef monitoring structures (ARMS). *Mol. Ecol.* 28, 3496–3507. doi: 10.1111/mec.15167

Pearman, J. K., Chust, G., Aylagas, E., Villarino, E., Watson, J. R., Chenuil, A., et al. (2020). Pan-regional marine benthic cryptobiome biodiversity patterns revealed by metabarcoding autonomous reef monitoring structures. *Mol. Ecol.* 29, 4882–4897. doi: 10.1111/mec.15692

Pearman, J. K., Leray, M., Villalobos, R., Machida, R. J., Berumen, M. L., Knowlton, N., et al. (2018). Cross-shelf investigation of coral reef cryptic benthic organisms reveals diversity patterns of the hidden majority. *Sci. Rep.* 8, 1–17. doi: 10.1038/s41598-018-26332-5

Peck, L., Clark, M., Power, D., Reis, J., Batista, F., and Harper, E. (2015). Acidification effects on biofouling communities: winners and losers. *Global Change Biol.* 21, 1907–1913. doi: 10.1111/gcb.12841

Pecquet, A., Dorey, N., and Chan, K. Y. K. (2017). Ocean acidification increases larval swimming speed and has limited effects on spawning and settlement of a robust fouling bryozoan, *Bugula neritina*. *Mar. pollut. Bull.* 124, 903–910. doi: 10.1016/j.marpolbul.2017.02.057

Pennesi, C., and Danovaro, R. (2017). Assessing marine environmental status through microphytobenthos assemblages colonizing the autonomous reef monitoring structures (ARMS) and their potential in coastal marine restoration. *Mar. pollut. Bull.* 125, 56–65. doi: 10.1016/j.marpolbul.2017.08.001

Pilly, S. S., Richardson, L. E., Turner, J. R., and Roche, R. C. (2017). Atoll-dependent variation in depth zonation of benthic communities on remote reefs. *Mar.Environ.Res.* 173, 105520. doi: 10.1016/j.marenvres.2021.105520

Porzio, L., Buia, M. C., and Hall-Spencer, J. M. (2011). Effects of ocean acidification on macroalgal communities. *J. Exp. Mar. Biol. Ecol.* 400, 278–287. doi: 10.1016/j.jembe.2011.02.011

Ransome, E., Geller, J. B., Timmers, M., Leray, M., Mahardini, A., Sembiring, A., et al. (2017). The importance of standardization for biodiversity comparisons: A case study using autonomous reef monitoring structures (ARMS) and metabarcoding to measure cryptic diversity on mo'orea coral reefs, French Polynesia. *PloS One* 12, e0175066. doi: 10.1371/journal.pone.0175066

R Core Team (2022). *R: A language and environment for statistical computing* (Vienna, Austria: R Foundation for Statistical Computing). Available at: https://www.R-project.org/.

Reid, E. C., DeCarlo, T. M., Cohen, A. L., Wong, G. T., Lentz, S. J., Safaie, A., et al. (2019). Internal waves influence the thermal and nutrient environment on a shallow coral reef. *Limnol. Oceanogr.* 64, 1949–1965. doi: 10.1002/lno.11162

Richter, C., Wunsch, M., Rasheed, M., Kötter, I., and Badran, M. I. (2001). Endoscopic exploration of red Sea coral reefs reveals dense populations of cavity-dwelling sponges. *Nature* 413, 726–730. doi: 10.1038/35099547

Rodolfo-Metalpa, R., Lombardi, C., Cocito, S., Hall-Spencer, J. M., and Gambi, M. C. (2010). Effects of ocean acidification and high temperatures on the bryozoan myriapora truncata at natural CO2 vents. *Mar. Ecol.* 31, 447–456. doi: 10.1111/j.1439-0485.2009.00354.x

Roth, F., Wild, C., Carvalho, S., Rädecker, N., Voolstra, C. R., Kürten, B., et al. (2019). An *in situ* approach for measuring biogeochemical fluxes in structurally complex benthic communities. *Methods Ecol. Evol.* 10, 712–725. doi: 10.1111/2041-210X.13151

Safaie, A., Silbiger, N. J., McClanahan, T. R., Pawlak, G., Barshis, D. J., Hench, J. L., et al. (2019). High frequency temperature variability reduces the risk of coral bleaching. *Nat. Commun.* 9, 1–12. doi: 10.1038/s41467-018-04074-2

Scheffers, S. R., de Goeij, J., van Duyl, F. C., and Bak, R. P. (2003). The cave-profiler: a simple tool to describe the 3-d structure of inaccessible coral reef cavities. *Coral Reefs* 22, 49–53. doi: 10.1007/s00338-003-0285-6

Scheffers, S. R., Van Soest, R. W., Nieuwland, G., and Bak, R. P. (2010). Coral reef framework cavities: Is functional similarity reflected in composition of the cryptic macrofaunal community? *Atoll Res. Bull.* 583, 1–24. doi: 10.5479/si.00775630.583.1

Sheppard, C., Sheppard, A., Mogg, A., Bayley, D., Dempsey, A. C., Roache, R., et al. (2017). Coral bleaching and mortality in the chagos archipelago. *Atoll Res. Bull.* 613, 1–26. doi: 10.5479/si.0077-5630.613

Steiner, Z., Turchyn, A. V., Harpaz, E., and Silverman, J. (2018). Water chemistry reveals a significant decline in coral calcification rates in the southern red Sea. *Nat. Commun.* 9, 1–8. doi: 10.1038/s41467-018-06030-6

Stewart, H. L., and Carpenter, R. C. (2003). The effects of morphology and water flow on photosynthesis of marine macroalgae. *Ecology* 84, 2999–3012. doi: 10.1890/02-0092

Steyaert, M., Mogg, A., Dunn, N., Dowell, R., and Head, C. E. (2022). Observations of coral and cryptobenthic sponge fluorescence and recruitment on autonomous reef monitoring structures (ARMS). *Coral Reefs* 41, 877–883. doi: 10.1007/s00338-022-02283-2

Storlazzi, C. D., Field, M. E., and Bothner, M. H. (2011). The use (and misuse) of sediment traps in coral reef environments: theory, observations, and suggested protocols. *Coral Reefs* 30, 23–38. doi: 10.1007/s00338-010-0705-3

Sura, S. A., Delgadillo, A., Franco, N., Gu, K., Turba, R., and Fong, P. (2019). Macroalgae and nutrients promote algal turf growth in the absence of herbivores. *Coral Reefs* 38, 425–429. doi: 10.1007/s00338-019-01793-w

Tebbett, S. B., Bellwood, D. R., and Purcell, S. W. (2018). Sediment addition drives declines in algal turf yield to herbivorous coral reef fishes: implications for reefs and reef fisheries. *Coral Reefs* 37, 929–937. doi: 10.1007/s00338-018-1718-6

Timmers, M. A., Jury, C. P., Vicente, J., Bahr, K. D., Webb, M. K., and Toonen, R. J. (2021). Biodiversity of coral reef cryptobiota shuffles but does not decline under the combined stressors of ocean warming and acidification. *PNAS.* 118, e2103275118. doi: 10.1073/pnas.2103275118

Timmers, M. A., Vicente, J., Webb, M., Jury, C. P., and Toonen, R. J. (2020). Sponging up diversity: Evaluating metabarcoding performance for a taxonomically challenging phylum within a complex cryptobenthic community. *Env. DNA* 4, 239–253. doi: 10.1002/edn3.163

van der Loos, L. M., and Nijland, R. (2021). Biases in bulk: DNA metabarcoding of marine communities and the methodology involved. *Mol. Ecol.* 30, 3270–3288. doi: 10.1111/mec.15592

Venables, W. N., and Ripley, B. D. (2002). Modern Applied Statistics with S. *Fourth Edition.* (New York: Springer)

Vicente, J., Webb, M. K., Paulay, G., Rakchai, W., Timmers, M. A., Jury, C. P., et al. (2021). Unveiling hidden sponge biodiversity within the Hawaiian reef cryptofauna. *Coral Reefs* 41, 727–742.

Wang, Y. I., Naumann, U., Wright, S. T., and Warton, D. I. (2012). Mvabund–an r package for model-based analysis of multivariate abundance data. *Methods Ecol. Evol.* 3, 471–474. doi: 10.1111/j.2041-210X.2012.00190.x

Warton, D. I., Wright, S. T., and Wang, Y. (2012). Distance-based multivariate analyses confound location and dispersion effects. *Methods Ecol. Evol.* 3, 89–101. doi: 10.1111/j.2041-210X.2011.00127.x

Wickham, H. (2016). *ggplot2: Elegant graphics for data analysis* (Verlag: Springer). Available at: https://ggplot2.tidyverse.org.

Williams, G. J., Gove, J. M., Eynaud, Y., Zgliczynski, B. J., and Sandin, S. A. (2015). Local human impacts decouple natural biophysical relationships on pacific coral reefs. *Ecography* 38, 751–761. doi: 10.1111/ecog.01353

Wizemann, A., Nandini, S., Stuhldreier, I., Sánchez-Noguera, C., Wisshak, M., Westphal, H., et al. (2018). Rapid bioerosion in a tropical upwelling coral reef. *PloS One* 13, e0202887. doi: 10.1371/journal.pone.0202887

Wyatt, A. S., Leichter, J. J., Toth, L. T., Miyajima, T., Aronson, R. B., and Nagata, T. (2020). Heat accumulation on coral reefs mitigated by internal waves. *Nat. Geosci.* 13, 28–34. doi: 10.1038/s41561-019-0486-4

Zimmerman, T. L., and Martin, J. W. (2004). Artificial reef matrix structures (ARMS): an inexpensive and effective method for collecting coral reef-associated invertebrates. *Gulf Caribb. Res.* 16, 59–64. doi: 10.18785/gcr.1601.08

Zweng, R. C., Koch, M. S., and Bowes, G. (2018). The role of irradiance and c-use strategies in tropical macroalgae photosynthetic response to ocean acidification. *Sci. Rep.* 8, 1–11. doi: 10.1038/s41598-018-27333-0